Physics – Uspekhi **42** (5) 481 – 503 (1999)

INSTRUMENTS AND METHODS OF INVESTIGATION PACS numbers: 03.65.Bz, **05.45.+b**, 05.70.Ln, 89.70.+c

An interference method for measuring atomic state parameters

Yu L Sokolov

Contents

Abstract. A new approach to the observation of the stationary interference pattern of atomic states is suggested. A number of experiments performed from 1970 to 1998 using various interferometer designs are described. Among these are the precision measurements of Lamb shift in the hydrogen atom and the discovery, in the course of this work, of a long-range interaction between the moving excited hydrogen atom and the metal surface.

1. Introduction

In the 1960s, especially in the latter half of the decade, a large number of experimental and theoretical papers appeared dealing with the effects caused by interactions between elementary particles occurring in bound states. The most important of these were concerned with the search for interactions involving neutral currents (note that the violation of parity in atoms caused by neutral currents was first considered by Ya B Zel'dovich as early as 1959 [1]). These investigations were actively pursued after the works of Glashow [2], Weinberg [3] and Salam [4], and eventually led to the discovery of the predicted interaction in experiments on the scattering of muon neutrinos by nucleons [5, 6].

In the same period, much attention in atomic physics and spectroscopy was paid to experimental and theoretical studies of the fine effects of interactions of bound particles, based on the interference of atomic states and the interference of quantum amplitudes of various processes. Worth mentioning among these are the beam experiments with a Stern – Gerlach interferometer [7, 8], studies of the Hanle effect [9, 10], the effect of crossing and anticrossing of levels [11], and the experiments much advanced in the early 1970s and based on the beam-foil technique — that is, charge exchange of fast ions on a thin carbon film (see the reviews [12 – 14]).

These studies accumulated extensive knowledge about the properties of bound states. In particular, it became clear that the energy of such a state can be extremely sensitive to the behavior of the interaction potential of particles at small distances.

Then, however, one may put forward a certain general concept: rather than building huge accelerators, increasing the energies and smashing deep into the particles, there is an alternative approach that may be more arduous, but at the same time more interesting and less expensive (in the monetary sense). We refer to the observations of various fine effects of bound states. Such observations are capable of detecting such small details of short-range interactions as would otherwise require very high energies. One may argue

Yu L Sokolov Russian Research Centre "Kurchatov Institute"
pl. Kurchatova 1, 123182 Moscow, Russian Federation
Tel. (7-095) 196-94 84
E-mail: lukich@qq.nfi.kiae.su

Received 15 July 1998, revised 29 January 1999
Uspekhi Fizicheskikh Nauk **169** (5) 559 – 583 (1999)
Translated by A S Dobroslavsky; edited by A Radzig

therefore that there is a special direction of study of elementary particles, based on very high precision measurements of the parameters of bound states.

What measurements then are the most accurate? Apparently, it is spectroscopic measurements, since they are essentially concerned with the amplitudes of transitions rather than the probabilities. What is more, the phases are extremely sensitive to all kinds of influences. This, however, is a philosophical matter that calls for separate treatment.

On the strength of the arguments developed above one might ask whether the conventional atomic physics could be turned into a kind of spectroscopy — treating atoms as waves and observing the interference of atomic states instead of observing the radiation. We shall then be dealing with the spectroscopy of atomic states rather than with the spectroscopy of waves emitted by atoms. Such a combination of two principles gives rise to a new direction: interference measurements of the parameters of bound states are used for finding the properties of elementary particles. For example, by measuring the Lamb shift in a hydrogen atom with a high accuracy [15] and comparing the result with the theoretical prediction, one can calculate the electrical radius of the proton.

The measurement of the Lamb shift δ in a hydrogen atom is known to be an important checkpoint of quantum electrodynamics (QED) at low energies. By the start of our work (1970), precision measurements of δ had been carried out for a long time (since 1953, see Ref. [16]), and nevertheless the progress in accuracy was quite modest, which could be attributed to the fundamental limitations of the traditional radiospectroscopic technique. At that time an agreement between theoretical and experimental values of δ seemed to have been achieved [17, 18]; at closer inspection, though, this agreement turned out to be dubious. The spread of the experimental values of δ was clearly too large to allow any reasonable comparison with the theory. On top of that, the spread of theoretical values was quite large as well. So it was not even clear to what cause one should attribute the discrepancy between $\delta_{\rm exp}$ and $\delta_{\rm th}$ — more likely to the errors in measurements and calculations than to the downfall of quantum electrodynamics.

After a comprehensive analysis of the situation, I came to the conclusion that the accuracy of the measurement of δ can be greatly improved by observing the interference of the 2S- or 2P-state of the hydrogen atom with an interferometer similar to the widely used two-beam optical interferometer. I considered several feasible schemes of such a device, and this is what came of it.

2. Principle of observing the interference of a selected atomic state

Imagine a beam of metastable $H(2S_{1/2})$ atoms passing through an electric field of strength E that is nonadiabatically terminated at the boundaries (Fig. 1). The criterion of nonadiabaticity is the condition that the flight frequency $\omega = v/d$ (where v is the velocity of atom, and d is the width of the region where the field grows or decreases) should be greater than or of the order of the Lamb frequency (for the transition $2S_{1/2}-2P_{1/2}$), or the fine-structure splitting frequency (for the transition $2S_{1/2}-2P_{3/2}$).

Upon crossing the boundary *1*, the atoms of the beam experience the perturbing influence of the growing field and pass into the superposition of eigenstates ψ_1 and ψ_2 with the

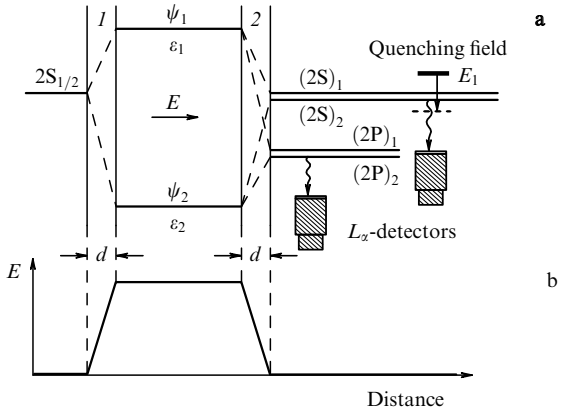

Figure 1. Scheme of an atomic interferometer (a) and a field strength profile (b).

energies ε_1 and ε_2 determined by the magnitude of the field E. On boundary *2*, where the field wanes to zero, components of the beam arise that represent both the state 2S and the state 2P, and each of the terms ψ_1 and ψ_2 gives rise to a pair of such states: $\psi_1 \to (2S)_1 + (2P)_1$, and $\psi_2 \to (2S)_2 + (2P)_2$.

Leaving the field, the amplitudes of 2S and 2P eigenstates will be determined by the amplitudes of transitions and the phase difference between the 'components' of each pair $(2S)_1 - (2S)_2$ and $(2P)_1 - (2P)_2$, which depends on the flight time in the field and the frequency of transition between the terms ψ_1 and ψ_2 split by the electric field. Since the magnitude of such a splitting depends wholly on the field strength E, a monotone variation of the field strength will give rise to periodic oscillations (in counterphase) of the intensity of fluxes of 2S and 2P atoms caused by the interference between $(2S)_1 - (2S)_2$ and between $(2P)_1 - (2P)_2$ 'components' in the outgoing beam. A similar pattern will be observed if the time of flight across the field is gradually varied by changing the distance between the boundaries *1* and *2*.

An interferometer based on this principle allows observation of the *steady* pattern of interference of the 2S or 2P state of hydrogen atom, thus making it possible to measure the parameters of this pattern with a high accuracy. Such an interferometer is rather similar to the two-beam optical one, where any individual photon interferes with itself. In our case, the 2S or 2P state of the atom interferes with itself. The interference is due to the fact that the resulting amplitudes of these states contain contributions caused by the evolution 'along different paths' — ψ_1 or ψ_2, which gives rise to a phase difference. It would be wrong to view the situation in such a way that the eigenstates 2S and 2P after evolution in the field of the interferometer are composed of the 'components' $(2S)_1$, $(2S)_2$, and $(2P)_1$, $(2P)_2$ — in reality these 'components' do not exist, and only serve to facilitate the understanding of the processes that take place inside the interferometer (in the same way as it would be wrong to speak of individual components of a photon having passed through the two-channel optical interferometer). The second 'channel' (ψ_2) in our atomic interferometer arises because the electric field mixes the states with opposite parity. In this way, the initial 2S state gets the coherent addition of the 2P state.

To forestall misinterpretation of Fig. 1, we ought to point out that the 'components' $(2S)_1$ and $(2S)_2$ have the same energy as do the 'components' $(2P)_1$ and $(2P)_2$. There is no

separation of the trajectories of 2S and 2P states either inside or outside of the interferometer.

The interference pattern of the 2P state can be registered by measuring the flux of L_α quanta that result from the radiative deexcitation of the short-lived 2P atoms ($\tau = 1.6 \times 10^{-9}$ s). The interference of the 2S state is recorded with the aid of a 'quenching' field E_1 (see Fig. 1).

If we set $x = \langle \mathrm{d} \rangle E/(\pi\hbar\delta)$, where $\langle \mathrm{d} \rangle$ is the matrix element of the $2S_{1/2}-2P_{1/2}$ transition, E is the field strength, and δ is the Lamb shift, then the appropriate analysis indicates (see Appendix I) that the yield of 2P atoms after a beam passage through the interferometer is proportional to the quantity

$$w(E, T) = \exp\left(-\frac{\gamma T}{2}\right) \times \left\{\frac{x^2}{1+x^2}\left[\cosh\frac{\gamma T}{2\sqrt{1+x^2}} - \cos 2\pi T\delta\sqrt{1+x^2}\right]\right\}, \quad (1)$$

where T is the time of flight in the field E, and γ is the decay constant of the $2P_{1/2}$ state (the hyperfine-structure splitting is not taken into account).

We see that the interference curve displays a mean curve defined by the hyperbolic cosine with the superimposed oscillating structure with a trigonometric cosine.

To simplify the analysis at the initial 'qualitative' stage, it will be worthwhile to divide the interval of the values of field strength E into the subregions of 'normal' and 'strong' fields. Normal fields are those for which the condition $x \sim 1$ holds — that is, which cause a Stark shift of levels $2S_{1/2}$ and $2P_{1/2}$ of the same order of magnitude as the Lamb shift. In the range of normal fields ($E \sim 200-300$ V cm^{-1}), the effects of the Lamb shift are especially clear; at the same time, the presence of the $2P_{3/2}$ level is of little consequence, which allows the problem to be reduced to the two-level system $2S_{1/2}-2P_{1/2}$. The effect of the $2P_{3/2}$ level in this case can be taken into account by introducing small corrections [3].

For one thing, the effect of this level consists in that the transition $2S_{1/2}-2P_{3/2}$ makes a certain contribution to the registered L_α radiation. With normal fields, however, the amplitude of such a transition is of the order of 0.1, which gives a correction to the measured intensity not greater than 0.01. In reality this correction will be even smaller, since the condition of nonadiabaticity in the range of normal fields and the existing geometry of electrodes of the interferometer is only well satisfied for the level $2P_{1/2}$, but not for the level $2P_{3/2}$.

The observed pattern of interference $I_{2P}(E)$ is a superposition of curves related to the transitions both to the level $2P_{1/2}$ and to the level $2P_{3/2}$. In our situation, oscillations of the latter curve will occur at a frequency that is $\nu_f/\delta \sim 10$ times as high, and with an amplitude that is no greater than 0.01 of the amplitude corresponding to the transition to the level $2P_{1/2}$ (here ν_f is the frequency of fine-structure splitting). Since in the experiment under consideration we are going to register the total radiation from the levels $2P_{1/2}$ and $2P_{3/2}$, we must add to the probability of yield of atoms in the state $2P_{1/2}$ the probability of yield of atoms in the state $2P_{3/2}$, which is given by a similar formula. Since the contribution of the level $2P_{3/2}$ exhibits periodical changes that at $E \sim 300$ V cm^{-1} appear as small fast oscillations with respect to the primary cosine wave, the calculation of the contribution from this level must include averaging over the fast oscillations whose frequency is close to the frequency of fine-structure splitting.

The attendance of the $2P_{3/2}$ level also has another, more important effect caused by the mutual perturbation of the states of the H atom in the electric field that have the same n and different l, which alters the Stark splitting of levels $2P_{1/2}-2P_{3/2}$. The resulting correction is also of the order of 0.01, but its effect is more substantial because this is a correction to the phase. For large flight times the correction to the phase may be as large as 1, which must be duly accounted for in the calculation of the function $I_{2P}(E, T)$.

If we take into account the hyperfine structure of the levels $2S_{1/2}$ and $2P_{1/2}$ (Fig. 2), then the theoretical interference curve derived from the analysis of the two-level system $2S_{1/2}-2P_{1/2}$, will result from the superposition of three curves corresponding to the transitions 1, 2, and 3 (the energies of transitions 3 and 3′ are the same). Accordingly, the intensity of the 2P component of the beam passed through the interferometer can be represented as

$$W = w_1 + w_2 + w_3 = \exp\left(-\frac{\gamma T}{2}\right) \times \left\{c_1\frac{x_1^2}{1+x_1^2}\left[\cosh\frac{\gamma T}{2(1+x_1^2)^{1/2}} - \cos 2\pi\left(\delta + \frac{2}{3}v\right) \times T(1+x_1^2)^{1/2}\right] + c_2\frac{x_2^2}{1+x_2^2}\left[\cosh\frac{\gamma T}{2(1+x_2^2)^{1/2}} - \cos 2\pi\left(\delta - \frac{10}{3}v\right)T(1+x_2^2)^{1/2}\right] + c_3\frac{x_3^2}{1+x_3^2}\left[\cosh\frac{\gamma T}{2(1+x_3^2)^{1/2}} - \cos 2\pi(\delta + 2v)T(1+x_3^2)^{1/2}\right]\right\}, \quad (2)$$

where

$$x_1 = x\Big/\left(1 + \frac{2}{3}\frac{v}{\delta}\right); \quad x_2 = x\Big/\left(1 - \frac{10}{3}\frac{v}{\delta}\right); \quad x_3 = x\Big/\left(1 + 2\frac{v}{\delta}\right),$$

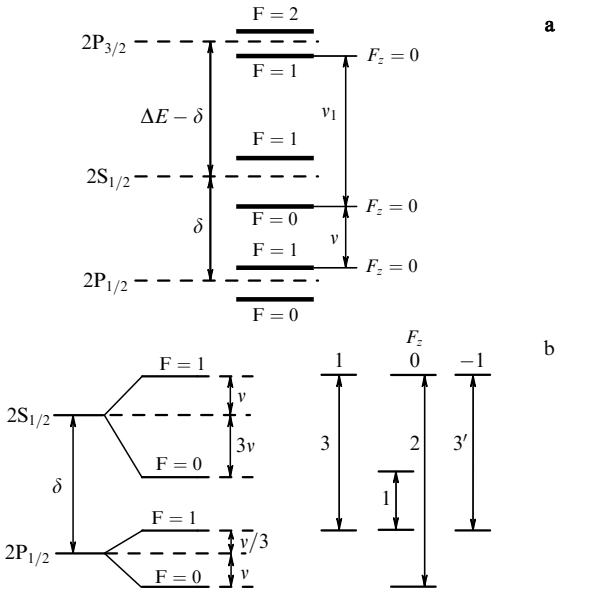

Figure 2. Scheme of $2S_{1/2}$, $2P_{1/2}$ and $2P_{3/2}$ levels of a hydrogen atom (a), and hyperfine structure of $2S_{1/2}-2P_{1/2}$ levels of a hydrogen atom (b).

ν is the frequency of hyperfine-structure splitting, and c_1, c_2 and c_3 are constants.

Hence it follows that by aligning the theoretical curve with the experimental one — that is, by adjusting the values of the coefficients c_1, c_2, c_3 (with the given Lamb shift, frequency of hyperfine-structure splitting and the time of flight through the interferometer), one can calculate the populations of sublevels of hyperfine structure of the $2S_{1/2}$ state with the projections of the total momentum F_z equal to 1, 0, and -1 (for $F = 1$), and $F_z = 0$ (for $F = 0$).

3. Evaluation of factors critical to the feasibility of the experiment

Notwithstanding the straightforward principle of the experiment for observing the interference of the 2P state of the hydrogen atom as illustrated in Fig. 1, its realization involved the design and construction of extremely sophisticated special equipment (just to mention the capability of measuring the Lamb shift to an accuracy of 2 ppm).

Serious problems associated with the staging of such an experiment stem primarily from the unusual and controversial requirements on the beam of 2S atoms passing through the interferometer (as shown in Fig. 1, the simplest interferometer is made up of two parallel plates — electrodes with holes for the beam). 'High purity' (free from foreign particles) beams of metastable hydrogen atoms with thermal velocities, generated with fairly well developed techniques [15], are totally unsuited to our purposes, since the interferometer would then have been of microscopic dimensions. It is only possible to construct the interferometer for the velocities of atoms of the order of 2×10^8 cm s^{-1}, which can be obtained by charge exchange of fast protons — for example, in a thin carbon film or in a gas target. However, even with such a value of velocity, it is only possible to create nonadiabatically varying fields when the width of slits in the electrodes for admitting the beam is not greater than a few tenths of a millimeter. Under these conditions, the field can only be assumed to be uniform over the cross-section of the strip-shaped beam when its transverse dimension (thickness) is not greater than 0.1 mm. In practice, however, one does not benefit from the increased dimensions of the beam and the interferometer, and respectively the increased velocity of atoms for the following reasons.

In the experiment proposed we measure the intensity of the 2P component of the beam, which, as described above, is accomplished by registering the quanta emitted in the course of the one-photon transition 2P – 1S, i.e. the resonance line L_α ($\lambda = 1216$ A). Because of this, the beam should not contain too many excited atoms whose cascade transitions to the ground state 1S could initiate the essential background and disguise the effects of interest. At the same time, the proton charge-exchange technique only produces a mixed beam of fast hydrogen atoms that occur in all possible states from $n = 1$ to $n \sim 15-20$. In order to create a suitable beam, one must first of all remove all short-lived atoms with $n = 2-6$, and the only way to do this is to give them enough time to radiatively release their energy. If the neutral hydrogen atoms are produced by proton charge exchange in a gas target, then the number of long-lived highly excited atoms in the beam will be rather small, because the population of levels with this technique falls off as n^3. Estimates indicate (see Appendix II) that an acceptable reduction of the background created by the excited atoms travelling at 2×10^8 cm s^{-1} may be achieved over a flight path of at least 200 cm. This value of velocity must be regarded as optimal, because then the interferometer is not too tiny, and the vacuum chamber is not too large.

To assure the stable velocity of protons that later become neutral atoms, we must use a velocity analyzer consisting of a magnet with a system of collimator slits [19].

The analysis of experimental data will be much facilitated if we remove from the beam the $2S_{1/2}$ atoms with total momentum $F = 1$. For this purpose the beam must be passed through microwave fields with frequencies 1147 MHz (for transition 2) and 1087 MHz (for transitions 3 and 3′). In this case the interference curve will result from the coherent mixing of states $|1\rangle \equiv |2S_{1/2},\ F = 0,\ F_z = 0\rangle$ and $|2\rangle \equiv |2P_{1/2},\ F = 0,\ F_z = 0\rangle$, corresponding to transition 1 with frequency 909.9 MHz (see Fig. 2). In this way, in place of the total pattern resulting from the superposition of the interference curves w_1, w_2, w_3, we shall only observe one curve w_3 [20].

Let us take a metal plate and
make a little metal hole in it.
M A Leontovich
(speaking at a seminar)

4. Atomic interferometer

Based on the above considerations, I designed my experimental apparatus and christened it 'Pamir', in honor of the mountains of Central Asia where my heart belongs.

The installation consisted of two main parts. One comprised the source of protons of energy 20 keV and the velocity analyzer consisting of a magnet which deflected the beam to an angle of about 80 degrees, with a system of collimator slits. The other (diagnostic) part, separated from the first by the gas target (charge-exchange chamber) where the protons were converted into neutral hydrogen atoms, included the interferometer and resonators that produced the microwave fields with frequencies 1148, 1087, and 909.9 MHz for quenching the components of the 2S state with total momenta $F = 1$, $F = 0$, and some instrumentation for monitoring the parameters of the beam.

At the time when I was ready to build my experimental system, I was working under I N Golovin at the thermonuclear facility called 'Ogra', a plasma trap with magnetic 'stops'. I was concerned with the diagnostics of plasma, and the injection of neutral hydrogen atoms. Frankly speaking, over the few years in this business I developed a highly skeptical attitude to the feasibility of thermonuclear reactors where the hot plasma was confined in magnetic fields. I may be wrong, but it looked like there was a universal theorem — still to be formulated and proved — that forbade the construction of such a reactor for steady generation of electric power. There is something preternatural in this idea, and the argument that these processes take place inside stars is hardly convincing, since the plasma in the stars is confined by stupendous forces of gravity.

I firmly made up my mind to steer clear of this thermonuclear affair, and to concentrate instead on my experiments on observing the interference of atomic states. The concept was discussed at length with I N Golovin, V M Galitskiĭ and E K Zavoiskiĭ (V M Galitskiĭ was especially enthusiastic, since we saw the possibility of experimental verification of a new and very profound physical theory put forward by him). Eventually I received approval for the construction of my installation, and within one year it was in place.

A good deal of time passed, however, before we were able to start our observations of interference. The complications were due to the low intensity of the flux of 2S atoms through the interferometer, especially when we turned on the fields that quenched the component with total momentum F = 1. In order to collect good experimental statistics we needed that the flow rate of 2S atoms in the beam measuring 0.05 by 2 mm across should be at least 10^9 s^{-1}. The appropriate experiments indicated that this intensity can only be achieved if the source of primary protons is capable of producing a thin beam with low angular divergence.

Such a source was constructed in a purely empirical fashion, by trial and error method, based on the widely used source with a microwave discharge that produced a stable in time beam of protons and was convenient enough in operation. The principle of the source was traditional, but the design (the shape of the HF discharge tube, the shape and arrangement of coils connected to the oscillator, and especially the device for extraction of ions) was novel and highly optimized. The source produced a beam of protons with an energy of about 20 keV, an angular divergence of the beam of 3×10^{-3}, and a current of up to 1.2 mA (the power of the HF oscillator was 100 W at a frequency of 30 MHz).

Three methods for obtaining neutral atoms were studied: charge exchange of protons in a thin carbon film (about 100 A thick), charge exchange in a gas target, and neutralization of protons by a superimposed beam of electrons travelling at the same speed. In those years (1968 – 1969) there were few results on the charge exchange of fast atoms in thin films, and so we had to tread the uncharted ground on our own. From the first successful experiments it became clear at once that the proton charge exchange on a film did not suit the purpose (long-term measurements with a highly stable atomic beam). The carbon films were rapidly destroyed, and were only good for short experimental runs; in addition, their thickness varied, which necessitated repeated calibration runs after each replacement. It should be noted that the beam-foil technique was much advanced in the 1970s in the arrangement when the ions left the foil after charge exchange in a coherent superposition of states, which led to spatial beating in the resulting luminescence [12].

Charge exchange of protons in a gas target was a well studied and widely used method for producing beams of fast hydrogen atoms. The best yield of metastable 2S atoms is achieved in cesium vapor. For our purposes, however, there was no need to use a cesium target, since relatively weak currents were sufficient for observing the interference, while the high stability of the atomic beam for several hours at a stretch was of utmost importance when operating continuously. The best results were obtained with the charge exchange chamber filled with molecular hydrogen and located 100 cm away from the analyzing magnet assembly. In this case, with the thickness of the gas target about 0.03 Torr $\times$ cm, the angular divergence of the beam of hydrogen atoms was $\sim 0.3 \times 10^{-3}$.

Studying the interaction of superimposed beams of protons and electrons moving at the same speed, we registered the appearance of hydrogen atoms in different excited states. In this experiment, the charge-exchange chamber was evacuated to a pressure of about 2×10^{-6} Torr, and the formation of neutral atoms resulted from the recombination of protons and electrons travelling at the same speed in the superimposed beams. Experimental data imply that in the case in question we are dealing not with radiation recombination (as had been initially assumed), but rather with recombination at triple collisions, which is more likely to populate the upper levels of the hydrogen atom.

The recombination coefficient for the case of low temperatures ($kT \ll E_i$, where E_i is the ionization energy) was calculated in Ref. [22]. The results implied that at sufficiently low temperatures ($T_e \sim 0.01$ eV) three-body recombination may just occur at values of N_e of the order of 10^8 cm^{-3}, which corresponds to the number density of electrons in a beam produced with a Pierce gun and multistage deceleration. The yield of 2S atoms, however, was of the same order of magnitude as the background resulting from the charge exchange of protons on the residual gas. Because of this, all further experiments used a beam obtained by the charge exchange of protons in the hydrogen target.

In staging the interference experiments I greatly benefited from having been trained as an optical physicist and mechanic of the highest qualification: I had to make all interferometers with my own hands as they were highly sophisticated devices that called for the ultimate degree of precision.

Two types of interferometers were built for the initial experiments: with the electric field directed crosswise and lengthwise with respect to the direction of velocity of atoms. The interferometer with the transverse field was used for studying the effect as a function of the field strength while the flight time T remained constant. A nonadiabatic change of the electric field on the boundaries in an interferometer of this type could be realized with substantial separation between the electrodes creating this field, which was important for a number of planned experiments. The interferometer with the longitudinal field (Fig. 3) permitted measuring both $I_{2P}(E)$ and $I_{2P}(T)$. In all cases, the interferometers were placed 200 cm away from the exit diaphragm of the charge-exchange chamber.

In the first experiments, as ought to be expected, the 2P component of the beam was registered, resulting from the 2S atoms having passed through the field of the interferometer. As the distance x between the detector and the boundary of the field was varied, the flow rate of the 2P atoms decreased monotonically as $\exp\left[-x/(v\tau)\right]$, where v is the velocity of atoms, and τ is the lifetime of the 2P state.

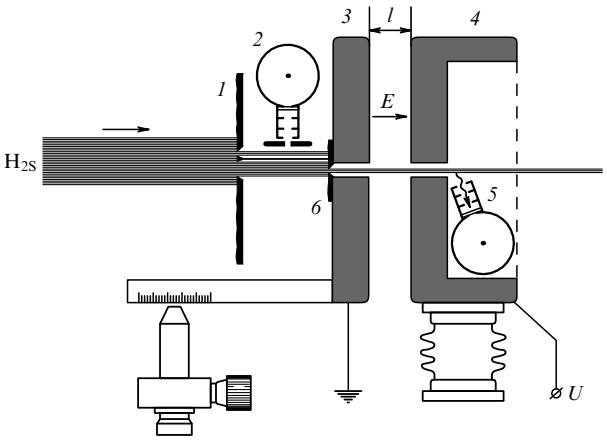

Figure 3. Scheme of the two-electrode interferometer with a longitudinal field: *1* — separating diaphragm; *2* — detector of the monitor; *3* and *4* — flat electrodes with slits for passing the beam; *5* — detector of the effect; *6* — collimator slit.

The interference curve depicting the dependence $I_{2P}(E)_{T=\text{const}}$, obtained with the interferometer with a longitudinal field, is shown in Fig. 4. Observe that the patterns shown in Fig. 4 are the optical analog of the effect predicted by Pais and Piccioni [23] for the system of K^0 and $\bar{K}^0$ mesons.

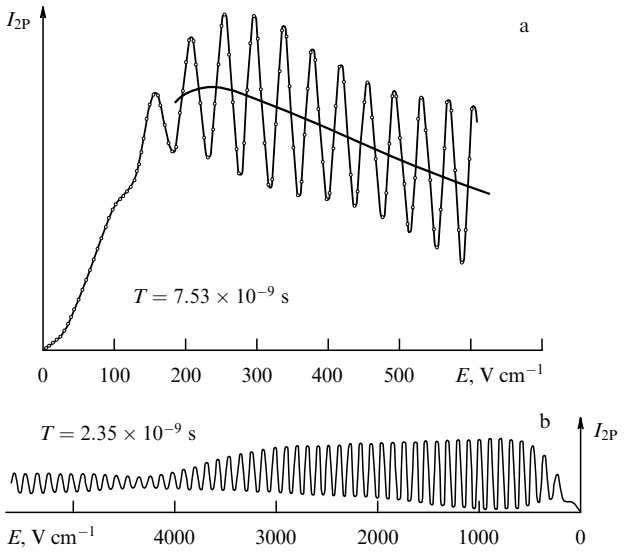

Figure 4. Interference pattern of the 2P beam components for the flight times $T = 7.53 \times 10^{-9}$ s (a), and $T = 2.35 \times 10^{-9}$ s (b).

The results obtained at the first stage of experiments using the above-described interferometers were published in Refs [19, 24].

As far as I know, my atomic interferometer, similar to the two-beam optical interferometer, was the first precision measuring instrument of this kind.

5. Galitskiĭ's theory

Immediately after the successful observation of interference of atomic states, we decided to embark on experimental verification of the theory of V M Galitskiĭ, putting off the measurements of the Lamb shift in atomic hydrogen, which was necessary both for improving the installation and for streamlining the procedures for precision measurements.

Unfortunately, Victor Mikhaĭlovich Galitskiĭ (1924–1981) has not left us any written account of his theory, not even as much as notes on the back of an envelope. Being a close acquaintance of Galitskiĭ, and talking of the planned experiments with him now and again, I had a clear feeling that he had thought it over very thoroughly, had worked out all aspects of his theory. To my questions why he would not discuss it in public, Galitskiĭ invariably answered: "Let us carry out our experiments, then we shall see what to do next". I am certainly unaware of having the right to act so but I believe that the extremely interesting ideas of Galitskiĭ should not perish in vain. The following is based on my shorthand notes made when our discussions were still fresh in my memory.

The conception of Galitskiĭ related to the structure of a theory that should describe the totality of physical observations. It was based on universal logical constructions, on the most general ideas, and can mainly be described as follows.

The contemporary picture of the physical world is based on two extreme constructions, known as classical and quantum mechanics. According to Galitskiĭ, all physical phenomena are actually embraced by a certain comprehensive unified theory, in which classical and quantum mechanics represent two distinct limits. The structure of this unified theory calls for certain additional terms (the 'reduction terms' in Galitskiĭ's terminology) which have the following property: if the microscopic phenomena are studied, then the main result is the Schrödinger equation with some deviations towards classical mechanics. Conversely, when the classical domain is studied, then the description is based on Newton's equations, with small corrections bearing the stamp of quantum mechanics.

In one of his letters to me Galitskiĭ explained his hypothesis in the following words: "Assume that there is classical mechanics and quantum mechanics. Now, I am not saying that there is something in between, some intermediate region. I say that there exists a general theory that covers everything, and whose one limit is classical mechanics, and the other limit is quantum mechanics. This is a very important point, since if there were an intermediate region, then for some reasons should not something from quantum mechanics go into classical mechanics, or vice versa? One of my most important assumptions is that there is no transition from quantum mechanics to the classical limit. This is what I am set to defeat."

Quantum systems obey the principle of superposition, whereas classical systems exist in the packet states — that is, superposition is not allowed. If this is so, then a similar property in one form or another should exist in quantum mechanics as well — otherwise there will be no way to quantum mechanics from the general theory.

Since classical motions occur as a mixture of states rather than a superposition, it follows that in nature there must be two opposing counterbalanced tendencies, one of which tends to preserve superposition, whereas the other seeks to destroy it and turn into a mixture — that is, to make the states non-interfering. The modified quantum theory must include certain additional terms accounting for such tendencies. These terms are small in quantum mechanics, but in the opposite limit of the unified theory — in classical mechanics — they become predominant. These additional terms 'work' very slowly. Because of this, as long as we are dealing with states with substantially different energies, the corresponding nonstationarity is hard to detect inasmuch as the observation is performed over a considerable length of time, and the observed effect is averaged. If, however, the observations are carried out under such conditions that beats are detectable (that is, when the difference in the energy of states is small enough), then the above-described trend may be quite noticeable.

From the purely logical considerations developed above it follows that if these processes actually exist in nature, then the short-lived component of a certain superposition cannot 'die out' completely because of the small 'classical' addition brought about by the reduction terms. This is a very important consequence. Consider, for example, the problem of violation of CP parity in the light of the Galitskiĭ theory.

Let us start with a brief summary. The invariance of weak interactions with respect to CP transformations implies certain properties of K^0 mesons. It turns out that if this symmetry is rigorous, then it is not the separate K^0 and $\bar{K}^0$ mesons that occur in the free state, but rather two types of superpositions of these particles with different lifetimes. In other words, in the beam we observe K_1^0 and K_2^0 mesons like

$$K_1^0 = \frac{1}{\sqrt{2}}(K^0 + \bar{K}^0), \quad K_2^0 = \frac{1}{\sqrt{2}}(K^0 - \bar{K}^0). \tag{3}$$

If we simultaneously apply the charge conjugation transform C and the space inversion P, we get the inversion $K^0 \to \bar{K}^0$ and $\bar{K}^0 \to K^0$. Then the particle K_1^0 converts into itself with phase conservation, i.e. its wave function will be even with respect to CP transformation. By contrast, the wave function of K_2^0 will change its phase and thus it will be odd.

Now let us see what happens when K_1^0 and K_2^0 decay to two charged π mesons. CP transformation converts these mesons one into the other, which means that they are particle and antiparticle. Because of this, the wave function of the π^+-π^- combination can only be CP-even. This implies that it is only K_1^0 that may decay to two charged pions; this is strictly forbidden for K_2^0.

The lifetime of a K_1^0 meson with respect to decaying to two pions is 0.88×10^{-10} s; the particle K_2^0 decays to three π^- mesons with the characteristic time 5.8×10^{-8} s. Such views on the properties of superposition (3) prevailed until 1964, when it was found that K_2^0 may also decay according to the forbidden scheme (in approximately one case out of 500).

This discovery gave rise to numerous assumptions concerning the possible causes of such a phenomenon, and eventually it was agreed that we are dealing with the violation of CP parity.

It ought to be noted, however, that the tacit assumption has always been that the superpositions (3) are obeyed rigorously; that once started they continue indefinitely, and that their short-lived components die and the long-lived remain. If we allow, however, that these superpositions are not perfect and that they contain a certain germ that seeks to destroy them, then our tentative corrections to the canonical quantum mechanics will bring about a situation when a certain concentration of K_1^0 is maintained in the beam — such that balances the two counteracting trends: one creating the superposition, and the other destroying it, i.e. turning it into a mixture. In such a case the experiments ought to detect the allowed decays $K_1^0 \to 2\pi$ observable at large distances, which could have been mistaken for the $K_2^0 \to 2\pi$ decays leading to the conclusion about violation of CP parity. Thus, if Galitskiĭ's hypothesis is correct, the entire phenomenon can be given a totally different explanation.

Obviously, the final settlement of the fundamental issue concerning the introduction of additional terms into the set of quantum mechanical equations depends on experiment. What then could be suggested as the crucial experiment?

A detailed study of superposition (3) can hardly lead to an unambiguous conclusion regarding the origin of the forbidden decay $K_2^0 \to 2\pi$, since this leaves two possible explanations: violation of CP parity, or violation of the principle of superposition.

More promising is the study of the superposition of 2S and 2P states of the hydrogen atom, whose energies differ by the magnitude of the Lamb shift. Let us consider in detail a possible realization of such an experiment.

Assume that a hydrogen atom in the state $2S_{1/2}$ passes through the interferometer shown in Fig. 1. The eigenstates ψ_1 and ψ_2 of the atom in the field of the interferometer are linear combinations of the states 2S and 2P:

$$\psi_+ = \frac{1}{\sqrt{2}}(\psi_{2S} + \psi_{2P}), \quad \psi_- = \frac{1}{\sqrt{2}}(\psi_{2S} - \psi_{2P}). \tag{4}$$

According to the canonical quantum mechanics, the state of the H atom after passing through the electric field will be described by the superposition

$$\psi = C_+\psi_+ + C_-\psi_-. \tag{5}$$

Let us see what will happen with this superposition from the standpoints of canonical and noncanonical quantum mechanics. The former implies that the states 2P must die out completely. This means that at large distances ψ must tend to ψ_{2S} — that is, if we take Eqn (4) into account, we have

$$\psi_{x\to\infty} \to \psi_{2S} = \frac{1}{\sqrt{2}}\psi_+ + \frac{1}{\sqrt{2}}\psi_-. \tag{6}$$

So, the canonical statement of quantum mechanics is as follows: firstly, this superposition must exist indefinitely long, and secondly, its coefficients will tend to the following values (with a certain common multiplier):

$$C_+ \to \frac{1}{\sqrt{2}}, \quad C_- \to \frac{1}{\sqrt{2}}. \tag{7}$$

The further statement, according to Galitskiĭ, consists in that there are certain corrections to quantum mechanics that work, on the contrary, to destroy this superposition and turn it into a mixture. Hence it follows (by analogy with the above case of K^0 mesons) that the 2P atoms cannot vanish completely, since this would imply the emergence of a rigorous superposition. Accordingly, the beam of hydrogen atoms having passed through the electric field ought to display a 'tail' of 2P atoms: at large distances the 2S atoms 'dislike' being alone and they start transforming into 2P atoms.

From the above it follows that the comprehensive quantum theory as applied to this experiment must include both the decay of 2P atoms and the effects of the corrections that tend to transform a superposition into a mixture. It is clear that the summands of both the types — the decay terms and reduction terms — work in opposite directions. To satisfy both, a compromise is required. Any kind of compromise implies, however, that there must be left 2P atoms in the beam, since their complete disappearance in no way indicates the compromise and would mean that everything goes to the decay and nothing to the reduction terms. If we assume then that the superposition turns into a mixture over a certain (long) time t, and if simultaneously the superposition persists over the lifetime τ, the compromise consists in that the beam contains an added number of 2P atoms $N_{2P} \sim \tau/t$. In the limit of a 'pure mixture' $|C_1|^2 = 1/2$ and $|C_2|^2 = 1/2$ (that is, if there were no interference and the proportion of 2P atoms in the case of no decay would have been 1/2), the beam would have become a mixture of 2S and 2P (more precisely, ψ_1 and ψ_2); if the decay had been taking place, the fraction of 2P atoms would have been zero. The transformation of a superposition into a mixture must occur over statistical times, i.e. about 10^{-4} to 10^{-5} s.

The phenomenon itself shows up as 2S atoms evolve 2P atoms through the characteristic time t, which die out with the characteristic time τ. Thus, the beam at any time contains only a small number of 2P atoms.

However, the experiment with the hydrogen atom contains an ambiguity, because it is not possible to tell in advance which degrees of freedom are involved in packetization. In

other words, there is not certainty as to what kind of mixture would have evolved in the absence of decays — with respect to ψ_1 and ψ_2, or to 2S and 2P. In principle, this ambiguity can easily be resolved: it is only necessary to produce a 'conflict' between packetization and the eigenstates. The experiment must be designed so that packetization in the zone of observation does not occur with respect to the eigenstates.

6. Attempt at experimental verification of Galitskiĭ's theory

Having considered thoroughly all the pros and cons concerning the study of the (2S – 2P) superposition of states of the hydrogen atom, we embarked on the experiments with the two-electrode interferometer with a longitudinal field and L_α detectors located at $x_1 = 10$ cm, $x_2 = 50$ cm, and $x_3 = 100$ cm.

The results were as follows. The detectors registered fluxes of 2P atoms that were slightly but consistently above the background. If Galitskiĭ's hypothesis is true, then the process of conversion of 2S atoms into 2P atoms (at a velocity of 2×10^8 cm s^{-1}) should be described by the exponential function $\exp(-1.2 \times 10^3 x)$. Observe that the accuracy of measurement of the characteristic constant of $2S \rightarrow 2P$ conversion was not better than 5%. Given this value of the conversion constant, it would seem worthwhile to stage an experiment aimed at direct measurement of the fadeout of the flux of 2S atoms in a nonadiabatic field with the detectors placed 10 to 20 meters apart.

The result obtained does not contradict the above basic considerations. At the same time, it cannot be taken for the unconditional proof of their validity: the small magnitude of the effect and the complexity of the experiment prompt us to treat the results with great caution.

What is more, the experiment suggests that we are dealing with packetization with respect to ψ_1 and ψ_2, even though one ought to expect it to involve the more 'classical' states 2S and 2P. It ought to be assumed, however, that packetization is likely to involve both ψ_1 and ψ_2 states, and the states 2S and 2P, with a certain associated probability.

In the second version of the experiment we observed the interference of 2P components of the beam, arising from the states ψ_1 and ψ_2 in the field of the interferometer. If packetization occurs with respect to states 2S and 2P, then the interference pattern will be distorted because of the destruction of superpositions $\psi_1 = (2S + 2P)/\sqrt{2}$ and $\psi_2 = (2S - 2P)/\sqrt{2}$. The short time of flight of atoms in the field of interferometer compared to the time of transformation $2S \rightarrow 2P$ does not give much confidence in the variations of the measured interference curve.

After the death of V M Galitskiĭ these experiments (owing to the impossibility of comparing the results obtained with the general theoretical predictions) and any further discussions of the possible causes of the 'tail' of 2P atoms, were discontinued.

7. Advancement of the technique: a 'double' interferometer

Our further work was concerned with the measurement of the Lamb shift in the hydrogen atom. I ought to mention that V P Yakovlev, a colleague of Galitskiĭ, was actively involved in the studies of atomic interference from the very beginning. He performed an exhaustive theoretical analysis of the processes taking place in interferometers of different designs. These experiments wholly relied on the techniques designed for the verification of Galitskiĭ's hypothesis.

If the goal consists in measuring δ to the accuracy of a few parts per million, then the precision of Eqn (1) is not sufficient. This is mainly because of the complexity of the atom's behavior in the interferometer, and the ambiguous boundary conditions — that is, the field pattern near the entrance and exit slits in the electrodes. In the course of discussion of the problem, Yakovlev suggested a way to get round these difficulties by making an interferometer consisting of two independent systems I and II, separated with a gap l (Fig. 5).

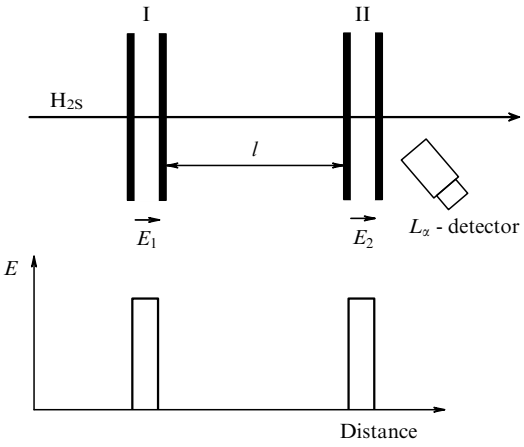

Figure 5. Scheme of the double interferometer.

The atom travelling at velocity v is subject to nonadiabatic electric fields in each system that mix the 2S and 2P states. In the gap between the systems — that is, in the region where the field is absent, the states 2S and 2P are eigenstates, and their evolution can be described exactly. This implies that we can write an exact expression for the probability $w(l)_{E_1, E_2}$ of yield of 2P atoms from the double interferometer as a function of the length l (or the flight time $T = l/v$), which would contain several parameters that take care of the fields E_1 and E_2. If the conditions in the two systems are kept the same while the distance l is varied, then these parameters are fixed, and one need not bother about calculating them [the number of these parameters can be reduced to one by appropriate treatment of the curve $w(l)$].

It is important that in the experimental determination of the function $w(l)$, the length l can be not the absolute length of the gap, but rather its increment counted from some arbitrary reference point. The final formula for the probability of yield of 2P atoms as a function of the flight length variation Δl is given by

$$w(\Delta l) = \cos\left[\frac{\omega}{v}\left(1 - \frac{v^2}{c^2}\right)^{1/2}\Delta l\right] + c\cos\left[\frac{\omega_1}{v}\left(1 - \frac{v^2}{c^2}\right)^{1/2}\Delta l\right]. \quad (8)$$

Here v is the velocity of atoms, c is the unknown parameter, $\omega = 2\pi\nu$, and $\omega_1 = 2\pi\nu_1$, where ν and ν_1 are the frequencies corresponding to the transitions shown in Fig. 2. The factor $(1 - v^2/c^2)^{1/2}$ takes care of the Lorentz contraction. It is obviously small but necessary for achieving the desired accuracy.

We see that this version of the experiment allows the ratio ω/v to be found. In this way, to obtain the Lamb shift it is necessary to take an independent measurement of the velocity of atoms v.

In accordance with the scheme just described, the technique was as follows:

1) with fixed electric fields in systems I and II and arbitrary distance between the systems (which is taken for $l_1 = 0$), find the number of L_α quanta resulting from the decay of the 2P state after passing through the systems I and II [that is, find $I_{2P}(l_1)$];

2) the direction of field in system II is reversed, other conditions being constant; the measurement gives the value of $I'(l_1)$;

3) find the difference $I - I'$;

4) field strength E_2 is brought back to its initial value; distance l is then changed by the amount Δl, and two measurements are taken for the opposing directions of the field — that is, the quantities $I(l_2)$ and $I'(l_2)$ are measured;

5) the same procedure is repeated for the selected sequence of increments Δl;

6) the measured values are used for plotting the experimental curve (8). The sought-for frequency of transition $2S_{1/2}$ $(F = 0,\ F_z = 0) \rightarrow 2P_{1/2}$ $(F = 1,\ F_z = 0)$ is found by fitting the theoretical curve to the experimental points — that is, by adjusting the values of ω/v and C.

As mentioned above, to find the Lamb frequency ν one needs an independent measurement of the velocity of 2S atoms. Stabilization and measurement of this velocity turned out to be the most difficult part of the experiment, and the main source of limitations of the method.

In principle, the velocity of 2S atoms can be measured by passing them through a quenching field and observing the L_α luminescence at a small angle to the path of the beam. Then the Doppler shift of the spectral line L_α can be used to find the velocity of atoms v.

This method was tested on the 'Pamir' experimental setup (we used a vacuum spectrometer with a one-meter diffraction grating with 1200 lines per millimeter). It turned out, however, that this technique is not capable of measuring the atomic velocity with the desired accuracy, mainly because of the low light-gathering power of the instrument. An additional error was brought about by the L_α emission caused by the cascade transitions of highly excited hydrogen atoms whose velocities are different from that of the atoms in the 2S state.

We also tried the technique of velocity measurement based on counting the number of interference maxima registered in unit time, when the field strength is linearly varied in the two-electrode interferometer. Notice that the effect of 'passage of bands' in the detector visual field is similar to the effect known in optics: when one of the mirrors in the Michelson interferometer is moved at a velocity v in the direction of the beam, the intensity of the interference pattern becomes a function of time: $I = I_0\ (1 + \cos 2\pi ft)$, where $f = vv/c$ is the modulation frequency. This method is quite promising; in our realization, however, it also failed to ensure the desired accuracy of measuring the velocity v.

Eventually, the measurement of the atomic velocity in all the experiments concerned with the Lamb shift was performed by observing the radiative deexcitation of 2P atoms produced from the 2S atoms in the nonadiabatic field.

As the detector is moved along the beam path, the intensity of L_α radiation as a function of the distance x metered from the arbitrary point of reference will vary as $I = I_0 \exp(-x/l_0)$, where $l_0 = v\tau$ (v is the velocity of the atom, and τ is the lifetime of the 2P atom). In this way, the velocity v (or, more precisely, the quantity l_0) can be calculated from the slope of the straight line $\ln I = \text{const} - x/l_0$. The appropriate measuring system will include two detectors, of which one (the monitor) is fixed, and the other is moved along the path of the beam.

At first sight it may seem that this method may be applied to the measurement of I by monitoring the light intensity at two points of the path of the beam, separated by distance x. This scheme, however, can only be used when we know in advance that the intensity of the radiation recorded decreases exponentially with x, and the parameters of the experiment remain constant all the time. In view of this, the method of two points cannot be used for measuring the velocity of atoms in the beam because the exponential dependence $I_{2P}(x)$ is assumed *a priori* and may be not true owing to the experimental inconsistencies (for example, velocity variations). It follows that the mandatory component of the analysis of experimental findings is the verification of the assumed linearity of the function in question. In addition, when the intensity is measured only at two points of the path, the experimental error in the distance measurement is a systematic one. When the measurements are carried out at many points, such errors become random, and it is possible to apply the statistical treatment by the method of least squares.

In accordance with such a statement of the problem, we developed the following technique. The intensity of L_α radiation was measured at several points along the beam path — that is, for discrete values of x_i. At each ith point we took n readings within equal (or gradually increasing) time intervals. Then the set of values $y_{il} = \ln I_{il}$ $(l = 1, 2, \ldots, n)$ corresponding to the theoretical dependence $\Psi = \alpha + \beta x$, where $\Psi = \ln I$, $\alpha = \ln I_0$, and $\beta = -1/l_0$, we found the empirical function (regression curve) $Y = a - bx$. Calculation of the coefficients a and b of the latter allows us to find l_0 and calculate its random error [25].

Figure 6 shows one of the versions of the 'Pamir' experimental installation, used for measuring the Lamb shift of the hydrogen atom δ (H, $n = 2$). Protons with an energy of about 20 keV, produced by the ion source *1*, were passed through the velocity analyzer consisting of magnet *2* and slit diaphragm *3* 0.02 cm wide. The dispersion of the magnet measured in the plane of the diaphragm was 163 eV cm^{-1}; accordingly, the energy spread of the passing protons was less than 3.25 eV, or $\sim 1.6 \times 10^{-4}$ of their energy.

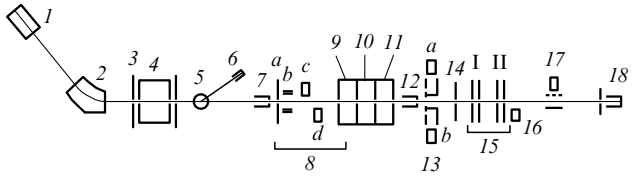

Figure 6. Scheme of the 'Pamir' installation (for explanations see text).

Neutral hydrogen atoms were produced in the charge-exchange chamber *4*. The combined beam was passed through a weak magnetic field *5*, which deflected the proton component (the proton current was measured with the Faraday cylinder *6*). The plane capacitor *7* was intended for 'quenching' the 2S atoms, which was necessary for finding the

level of the background. The velocity of atoms was measured with the assembly *8* consisting of the collimator slit *8a* and the transverse-field interferometer *8b* equipped with fixed detector (monitor) *8c* and movable detector *8d*. When not in operation, assembly *8* was removed from the beam path.

Microwave resonators *9 – 11* were tuned to the frequencies 1147, 1087 and 909.9 MHz. The first two removed the component of the 2S state with the total momentum $F = 1$ from the beam; the third resonator 'quenched' the component with $F = 0$ and was used for control measurements, in the course of which the 'quenching' field *12* (similar to field *7*) was used when the occasion required.

Further on the beam passed through differential monitor *13* with detectors *13a* and *13b*. Beyond the monitor *13* was the collimator slit *14* that formed a strip-shaped beam 0.05×2 mm, which then passed through the 'double' interferometer *15* with the L_α detector *16*. Assembly *17* with the transverse 'quenching' field was used for measuring the flux of 2S atoms. The total current of the beam was measured with the end gauge *18* by the secondary emission of electrons.

Figure 7a shows the system for measuring the velocity of atoms with the collimator slit *8a* (see Fig. 6). The slit consists of two elements: the precollimator covered with Aquadag or platinum sponge, and the collimator slit itself. The precollimator reduced the L_α background resulting from the excitation of atoms of the beam by secondary electrons produced by the beam hitting metallic surface. Here *1*, *2*, *3* are the electrodes creating the transverse field, *8c* is the fixed detector (monitor), *8d* is the movable detector, *4*, *5* are lenses made from lithium fluoride, and *6* is the screen grid [26].

Figure 7b shows the scheme of differential monitor *13* with the detectors *13a* and *13b* (see Fig. 6). The role of precollimator is played by the ribbed front wall coated with platinum black [25]. The use of a precision monitor was mandatory because the flux of 2S atoms was not constant,

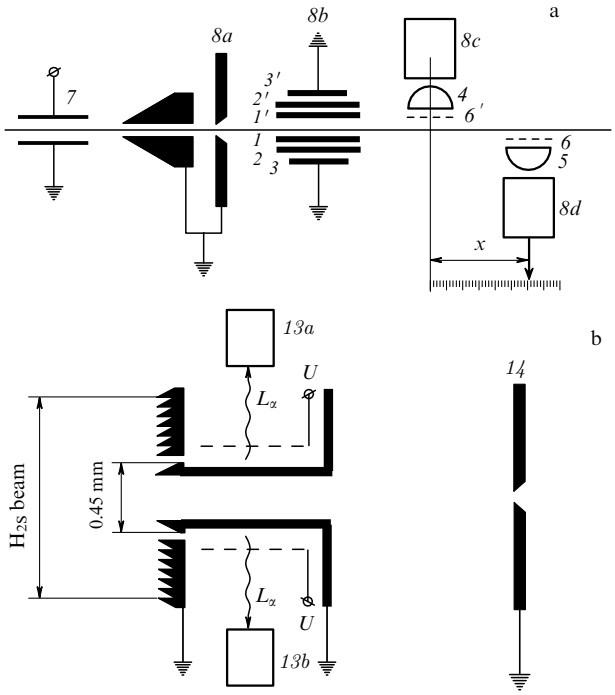

Figure 7. Schemes of device for measuring the velocity of atoms (a) and differential monitor (b) (for explanations see text).

and varied within about 0.3% over two hours. The main cause of instability was the frequency drift of microwave generators *10* and *11* (see Fig. 6) (the components of hyperfine structure of the L_α line overlap considerably; because of this, the detuning of resonators with the frequencies 1147 and 1087 MHz gives rise to variations of the intensity of the flux of 2S atoms with $F = 0$).

Figure 8a shows the practical scheme of the double interferometer. The electrodes *1*, *2*, *3* form the first (entrance) system, where the superposition $2S - 2P$ is created. The electrodes *4* and *5* form the second system (analyzer) with the detector *7* placed in the counting chamber 6, which is integral with the electrode *5*. The first assembly is moved with respect to the analyzer using a precision mechanism; the displacement (that is, the change in *l*) can be measured on the dial *8* using the same device as in an Abbe comparator, with an accuracy as good as 0.2 μm. Figure 8b shows a photograph of the double interferometer.

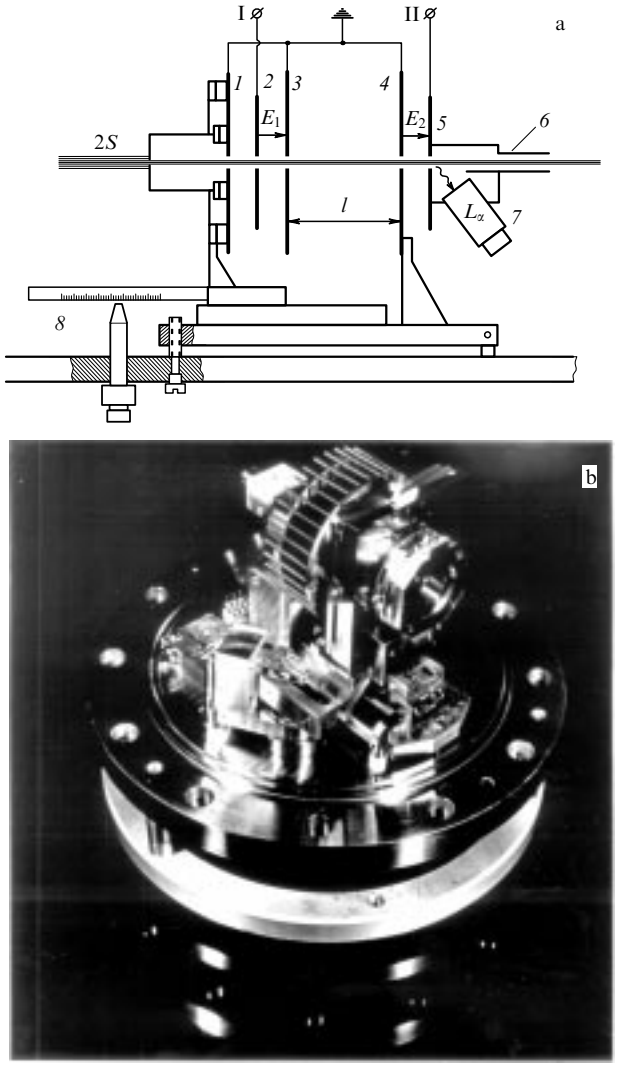

Figure 8. Scheme of double interferometer (a) and a photograph (b).

The thick-wall vacuum chamber which housed the interferometer was made of Armco iron. Specially staged experiments did not reveal any effects of external magnetic fields on the interference pattern.

The most difficult part of the experiment concerned with the measurement of the Lamb shift was the stabilization of the velocity of atoms (primary protons) to within 2 parts per million. The constancy of velocity of protons passing through the charge-exchange chamber *4* (see Fig. 6) depended on the constancy of their path (selected by magnet *2*) with respect to slit *3*. The path can be distorted by the temperature drift of characteristics of all the elements forming the atomic beam, including thermal deformations of the vacuum chamber. For eliminating the drift of proton velocity we used a specially designed power supply for the coils of magnet *2* that brought about the velocity drift of opposite sign, compensating the thermal drift of the system. In this way we were able to stabilize the velocity of 2S atoms to within 2 or 3 ppm over about two hours, which was enough for completing the measurements.

Over two years we made about 350 measurements of the Lamb shift. Only 42 of them passed the reliability test, mostly concerned with the constancy of the velocity. These 42 cases fall into a compact group shown in Fig. 9, where we have also indicated the value of the measured frequency of transition $2S_{1/2}\,(F=0\,,\ F_z=0)-2P_{1/2}(F=1\,,\ F_z=0)$ and the magnitude of the Lamb shift [25, 27]. The error in δ is the error of a single measurement. Formally, we ought to divide this by the square root of the number of measurements, that is, by $\sqrt{42}$. In such a case, however, the statistical error would have been 0.00025 MHz, which is less than the resolution threshold of our 'Pamir' installation, equal to 0.0011 MHz (since we were measuring the ratio of the Lamb shift to the velocity of atoms, the resolution threshold could be set by slightly adjusting the velocity).

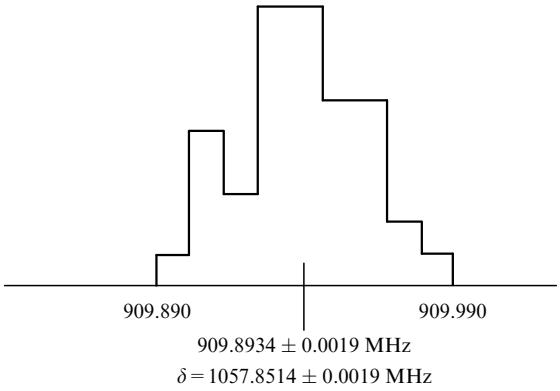

Figure 9. Histogram of measured values of the frequency of the 2S–2P transition.

Finally, it ought to be mentioned that the precision of our measurements of δ allows us to find, through comparison with $\delta_{\rm th}$, the electrical radius of the proton to an accuracy of 0.007 F; this is approximately one-second that from the measurements of (*e-p*) scattering at high energies [28].

We ought to mention that all measurements of the Lamb shift were made with the active participation of V G Pal'chikov, who, among other things, performed a highly accurate calculation of the lifetime of the hydrogen $2P_{1/2}$ state [28, 29], which was necessary for calculating the velocity of the atom. The feasible accuracy in the measurements of δ with an atomic interferometer is discussed in detail in Ref. [26].

8. Two-electrode interferometer

As indicated above, in the measurements of the Lamb shift the recommended procedure of treatment of experimental data (selected from several available options) required that two measurements should be made for each value of l in the registration of the flux of 2P atoms leaving the field E_2 (see Fig. 5 and System II in Fig. 6) — for the direct and inverse direction of the electric field with respect to the atoms' velocity. The criterion of proper operation of System II, which is the two-electrode interferometer as described above (see Figs 1 and 3) is the independence of the yield of 2P atoms from the sign of E_2 field, provided that only the atoms in the pure 2S state get into that field (this happens when the field E_1 is turned off). This is due to the simple fact that the electric field mixes the states with the opposite parity. Because of this, if an atom entering the interferometer is in the state with a given parity (for example, 2S), the probability of yield in the state 2S or 2P does not depend on the sign of the field. If, however, the initial wave function is a superposition of states with different parity (2S and 2P), then such probabilities for the opposite signs of the field differ by an amount proportional to the product of amplitudes of the atomic states 2S and 2P in the initial wave function. The method of measurement using fields of opposite signs can be employed, in particular, for finding a small addition of the 2P state to the initial state of the atom.

Working with the setup shown in Fig. 6, we had all grounds to assume that the atoms enter the interferometer in the pure 2S state. However, the control experiments done with the separate two-electrode interferometer (i.e. System II) revealed that the yield of 2P atoms depends on the direction of the field — the interference curves $I_{2P}(E_2)$ were not the same for the opposing directions of the field (Fig. 10). Because of this, in the measurements of the Lamb shift we selected such values of the field strength E_2 that corresponded to the intersections of the interference curves (+) and (○), where the equal yields of 2P atoms with field reversal could be ensured with the required accuracy.

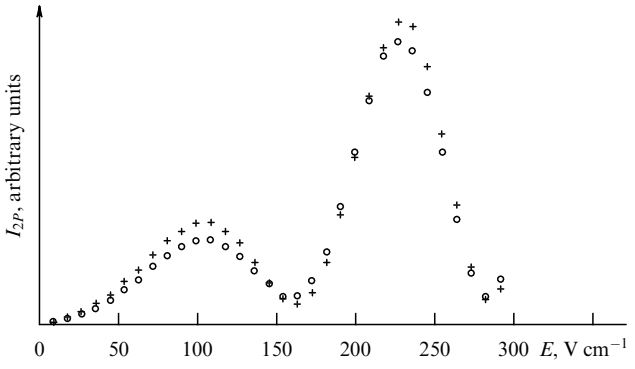

Figure 10. Interference curves for opposite directions of the field.

Now the question is what is the cause of dissimilarity of the interference curves, when the field E_2 is reversed. In this connection, the principle of the two-electrode interferometer was considered in detail in Ref. [30]. We confined ourselves to the simple case when the velocity of the H atom is constant and directed along the electric field, and the transitions to the state $2P_{3/2}$ can be disregarded. It was also assumed that the

beam only contained the 2S-state component with total momentum F = 0 — in other words, the problem reduced to a two-level system, where the electric field mixes the states $|1\rangle \equiv |2S_{1/2}, F = 0, F_z = 0\rangle$ and $|2\rangle \equiv |2P_{1/2}, F = 1, F_z = 0\rangle$. Then, in the proper reference frame ($z = vt$), the behavior of internal degrees of freedom of the atom is described by the following equations for the elements of the density matrix ($h = 1$):

$$\rho(t) \equiv \begin{vmatrix} \rho_{11}(t) & \rho_{12}(t) \\ \rho_{21}(t) & \rho_{22}(t) \end{vmatrix},$$

$$i\frac{\partial \rho_{11}}{\partial t} = V_{12}(t)\rho_{21} - V_{21}(t)\rho_{12},$$

$$i\left(\frac{\partial}{\partial t} + \gamma\right)\rho_{22} = V_{21}(t)\rho_{12} - V_{12}(t)\rho_{21},$$

$$\left[i\left(\frac{\partial}{\partial t} + \frac{\gamma}{2}\right) + \Delta\right]\rho_{21} = V_{21}(t)(\rho_{11} - \rho_{22}), \quad \rho_{12} = \rho_{21}^{*}. \quad (9)$$

Here $\Delta = E_{2S_{1/2}} - E_{2P_{1/2}} = 2\pi\nu$ is the Lamb splitting (for the transition in question $\nu = 909.8934$ MHz), $V_{21}(t) = \langle 2|\hat{d}_z|1\rangle$, $E(z = vt) = -\mathrm{d}E(t)$; the function $E(z)$ describes the field profile in the interferometer and is nonzero in a certain restricted space with the characteristic linear scale l (therefore, the flight time is $\tau = l/v$).

Without compromising generality, the matrix element $\mathrm{d} \equiv \langle 2|\hat{d}_z|1\rangle$ of the dipole transition may be considered real, and $V_{21}(t) = V_{12}(t) = V(t)$. Then the set of equations (9) becomes

$$i\frac{\partial \rho_{11}}{\partial t} = V(t)(\rho_{21} - \rho_{12}),$$

$$i\left(\frac{\partial}{\partial t} + \gamma\right)\rho_{22} = V(t)(\rho_{12} - \rho_{21}),$$

$$\left[i\left(\frac{\partial}{\partial t} + \frac{\gamma}{2}\right) + \Delta\right]\rho_{21} = V(t)(\rho_{11} - \rho_{22}), \quad \rho_{12} = \rho_{21}^{*}. \quad (10)$$

The state of atoms after passing through the interferometer (that is, where there is no field, $V = 0$) is assessed from L_α radiation whose intensity is proportional to ρ_{22} — the probability of population of the $2P_{1/2}$ state.

The result of analysis related to the dependence of population of sublevels of the 2P state on the sign of the field (that is, the dependence of ρ_{22} on the sign of V) is as follows: if the initial density matrix features some coherence between the states of different parity (that is, 2S and 2P), then the populations after the interaction will not have a predetermined parity with respect to the sign of the field, and so the flux of 2P atoms will change when E is replaced with $-E$. The measured value of ρ_{22} gives a direct indication of the initial coherence of the states 2S and 2P. In this way, by measuring the difference in the yield of 2P atoms when the field is reversed, we directly find the amplitude of this coherence. For a rectangular field profile it is easy to calculate $\rho_{22}(t)$ and find the magnitude and the phase of the initial coherence from comparison with the experiment.

9. The effect caused by field reversal in System II

The experimentally established asymmetrical yield of 2P atoms upon field reversal in the interferometer indicates that, prior to interaction with this field, the atom featured some initial coherence between the 2S and 2P states (in terms of the density matrix this implies that the off-diagonal element ρ_{21} is nonzero in the initial state; in terms of the wave function this means that the initial state of the atom is a superposition of the 2S and 2P states).

The question now is how and where, in which portion of the experimental installation shown in Fig. 6, could this coherence have started — that is, the superposition of the 2S and 2P states.

The asymmetry of yield of 2S and 2P atoms with respect to field reversal was studied in detail using the same experimental setup. In the first version we removed System I altogether, and performed all measurements with the two-electrode System II equipped with detector *16*.

In the absence of an external field, as follows from Eqn (10), the coherence $\rho_{21}(t) \sim \exp(-\gamma t/2)$ relaxes at the rate of $\gamma/2$ — that is, over a length of about $2v/\gamma = 0.6$ cm (given the velocity of atoms of 2×10^8 cm s^{-1}). Hence it follows that the source of coherence must be somewhere near the interferometer field, and must be independent of this field. As a matter of fact, it is the interference curve $I_{2P}(E)$ of the yield of 2P atoms as a function of field strength which is registered in the experiment, whereas the 'source' only produces the initial coherence ρ_{21}. The fact that by adjusting the absolute value and the phase of ρ_{21} in the initial state we can bring the intricate theoretical curve into coincidence with the experimental points over a broad range of field strength E (from 0 to 300 V cm^{-1}) is another obvious indication that the 'source of coherence' is not associated with the intrinsic field of the interferometer. Then the only reasonable assumption is that the 'source' is associated with the entrance slit of the interferometer (or with both slits). In other words, the passage of the atom through the slit in the first electrode gives rise to the coherence between the 2S and 2P states (superposition of the states) as a result of an interaction of some kind. Indeed, in the space before the entrance slit of the interferometer *15* (see Fig. 6) — that is, after leaving the collimator slit *14* — the atoms travelled along a very clean gold-plated liner free from any electric fields. The collimator slit itself also could hardly affect the results of the experiment, since it was located 3.25 cm away from the entrance slit. This means that if for whatever reason the superposition had developed on the slit *14*, then its 2P component at the entrance to the interferometer would have been reduced by a factor of 27500.

The surmised effect of the metallic slit on the passing 2S atoms was confirmed by a direct experiment (Fig. 11).

In this figure E_1 and E_2 are the 'quenching' fields, *1* is the collimator slit, *2* is the subject slit similar to the entrance slit of the interferometer, *A* and *B* are the L_α detectors, and *3* is the end gauge measuring the beam current.

Detector *A* was equipped with a replaceable collimator which selected a portion of the beam 1 to 6 mm long. The distance z between the window of a collimator and the slit could be varied from 2 to 10 mm. A number of experimental

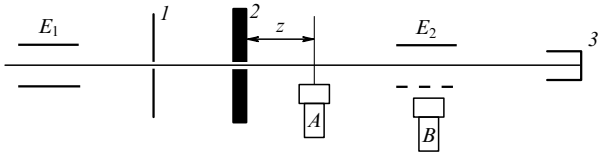

Figure 11. Scheme of the experiment with a single slit.

runs with different parameters of the setup revealed that the L_α background created by 2S atoms of the beam leaving slit *2* was about 30 times larger than without the slit.

As the distance z was increased, the intensity of L_α radiation decreased exponentially as $\exp[-\delta z/(v\tau)]$, where τ was found to be 1.55×10^{-9} s, which agrees well with the lifetime of the 2P atom.

Now what is the gist of these experiments? The 'background' measurements imply that the relative population of 2P states is $\sim 7 \times 10^{-4}$, which within 20% agrees with the results inferred from the interference curves, for which this value is 9×10^{-4}. The concordant results of the 'background' and interference measurements supply complementary information on the interaction of 2S atoms with the metallic slit. The 'background' measurements indicate that atoms in the 2P state are produced in the slit from the initial 2S atoms, and the interference experiments prove positively that a superposition of 2S and 2P states develops in the slit [30, 31].

The following circumstance ought to be pointed out. For the sake of simplicity, in all discussions so far we have been considering the effects of only the entrance slit of the interferometer. It is obvious that the exit slit will have a similar effect on the behavior of atoms, causing additional mixing of the 2S and 2P states. For a weak disturbance, the two slits give additive contributions to the interference curve. The resulting asymmetry depends, of course, not only on the magnitudes but also on the phases of the two contributions. Because of this, the net effect depends on the time of flight through the interferometer — that is, on the energy of the atoms. Figure 12 shows curves that picture the function $I_{2P}(E)$ upon field reversal for the energies of 17 and 26.5 keV (with the length of flight equal to 5 mm).

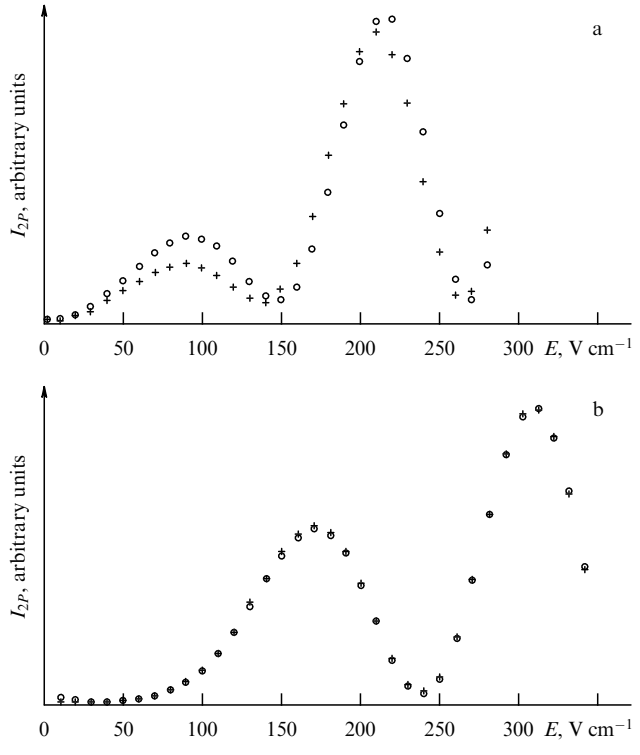

Figure 12. Interference curves for the energies 17 keV (a), and 26.5 keV (b).

We write what we observe; what we do not observe we do not write.
Admiral Stepan Makarov

10. Experimental studies of the interaction of the hydrogen atom with a metallic surface

10.1 Action of longitudinal and transverse fields

The phenomenon of 'slit' interaction was totally inexplicable. To prove its reality, we had to analyze the physical processes and the purely hardware effects that could have resulted in the (2S – 2P) superposition or its simulation — that is, to have caused a change in the flux of L_α quanta upon the reversal of electric field in the interferometer.

We considered several possible causes of the asymmetry in the intensity of the atomic beam radiation with respect to the replacement of E with $-E$ — such as, for example, the interference of two channels of decay (the electric dipole transition E1 from the 2P state, and the magnetic dipole transition M1 from the 2S state), the interaction of the quadrupole moment of the atom with the field gradient on the boundary of the interferometer, the 'cutoff' of the wave function by the edges of the slit, the perturbation of the atoms by thermal photons at the Lamb frequency, and the like. In all these cases, however, the estimated magnitudes of the effects were several orders of magnitude smaller than the experimental values.

One of the mechanisms that could produce the (2S – 2P) superposition in the slit may be the interaction of 2S atoms scattered by the collimator slit with its surfaces — that is, those atoms that form the halo of the beam. To check this assumption we performed two experiments with the setup shown in Fig. 6. In the first experiment, we removed System I and used System II and detectors *16* and *17* to obtain the interference patterns of 2S and 2P components of the beam — that is, to plot the functions $I_{2S}(E)$ and $I_{2P}(E)$. If the effect in question had been produced by the halo of the beam — that is, by a small portion of the flux of 2S atoms that had interacted with the slit surfaces — then the main beam of the atoms would have remained undisturbed, and would have completely hidden the effect produced by the minor halo. The interference curves, however, indicated that the slit had acted on all the 2S atoms of the beam (the second experiment is described in Section 10.4).

As pointed out above, the effect of the metallic slit on the atomic states is similar to that of the constant electric field. This experimental finding can form the base of a phenomenological description of interaction between the atoms and the slit, treated as the interaction with a certain effective 'electric' field. The magnitude and direction of such a field are free parameters found from comparison with the experimental interference curve.

Such a phenomenological theory, however, does not answer the main question: what is the physical mechanism of interaction between the atoms and metal. To answer this question, it would be desirable to supply System II with various devices producing fields of varying strength and orientation, thus simulating interaction with the slit. This could give some insight into the nature of such an interaction.

Hence it is necessary to analyze the conditions of arising interference of 2S and 2P states, when the atom in polarizer I and analyzer II is subject to the constant electric fields E_1 and E_2, which may have different (arbitrary) orientations with

respect to each other. It will obviously suffice, however, to consider two cases, when the fields E_1 and E_2 are parallel or perpendicular to the direction of the velocity of atoms.

a) *The case of parallel* (*longitudinal*) *fields*

The direction of the parallel fields E_1 and E_2 is selected for the z axis (the axis of quantization). Figure 13a shows the scheme of hyperfine structure of $2S_{1/2}$ and $2P_{1/2}$ states of the hydrogen atom; double arrows indicate the states for which the matrix elements of the operator of dipole moment d_z are nonzero (for the sake of simplicity we disregard the $2P_{3/2}$ component of the fine structure, which is justified when the fields are not too strong).

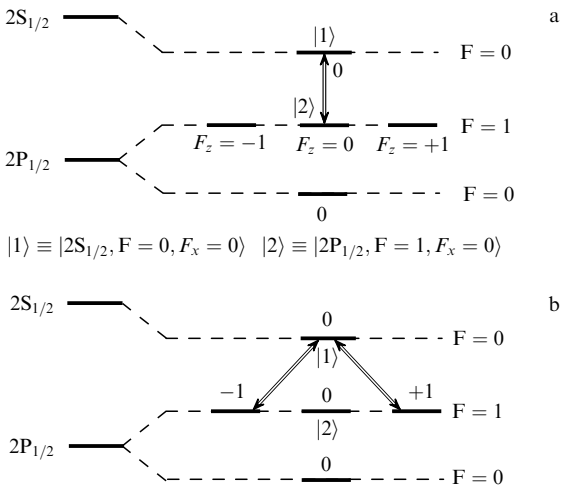

Figure 13. Mixing of states 2S – 2P, caused by longitudinal (a) and transverse (b) fields.

In the case of parallel fields E_1 and E_2, in each of the Systems I and II there is mixing of one and the same pair of states shown in the diagram with double arrows. If, as noted above, the component of hyperfine structure of the $2S_{1/2}$ state with total momentum F = 1 is removed from the atomic beam, then the interaction with the polarizer and analyzer only involves the pair of states

$$|1\rangle \equiv |2S_{1/2}\,,\ F = 0\,,\ F_z = 0\rangle\,, \quad |2\rangle \equiv |2P_{1/2}\,,\ F = 1\,,\ F_z = 0\rangle \tag{11}$$

(the corresponding transition is indicated in the diagram with a double arrow).

The z axis (the direction of parallel fields) can have an arbitrary orientation with respect to the atomic velocity v. Of practical interest, however, are the two cases when the z axis is either collinear or perpendicular to the velocity v. Atoms entering the polarizer reside in the state $|1\rangle$. After passing through the electric field E_1, the atoms occur in the superposition of states $|1\rangle$ and $|2\rangle$:

$$|1\rangle \to a_1|1\rangle + a_2|2\rangle\,. \tag{12}$$

There is no perturbation between Systems I and II, and the coefficients of superposition evolve freely — that is, one gets

$$a_1(t) = a_1\,, \quad a_2(t) = a_2 \exp\left(\mathrm{i}t\Delta - \frac{\gamma t}{2}\right), \tag{13}$$

where $\Delta = 2\pi\nu$, $\nu = 909.8934$ MHz, and $\gamma = 0.62646 \times 10^8$ s^{-1} is the radiation width of the 2P level. This presentation corresponds to measuring the energy from the energy of state $|1\rangle$. Then at the entrance to System II the state is

$$a_1(L)|1\rangle + a_2(L)|2\rangle\,, \quad L = vt\,,$$
$$a_1(L) = a_1\,, \quad a_2(L) = a_2 \exp\left(\mathrm{i}\frac{L\Delta}{v} - \frac{\gamma L}{2v}\right). \tag{14}$$

In System II under the action of field E_2 once again there is a mixing of states $|1\rangle$ and $|2\rangle$ — each of them becomes a superposition

$$|1\rangle \to b_1|1\rangle + b_2|2\rangle\,,$$
$$|2\rangle \to b_2'|1\rangle + b_1'|2\rangle\,. \tag{15}$$

Substituting Eqn (15) into Eqn (14), we find that the state of the atom at the exit of the interferometer is

$$C_1(L)|1\rangle + C_2(L)|2\rangle\,,$$
$$C_1(L) = a_1(L)b_1 + a_2(L)b_2'\,,$$
$$C_2(L) = a_1(L)b_2 + a_2(L)b_1'\,. \tag{16}$$

The populations of states $|1\rangle$ and $|2\rangle$ are given by

$$w_1(L) = A + B\exp\left(-\frac{\gamma L}{v}\right) + C\exp\left(-\frac{\gamma L}{2v}\right)\sin\left(\frac{L\Delta}{v} + \varphi\right),$$
$$w_2(L) = D\exp\left(-\frac{\gamma L}{v}\right) + E\exp\left(-\frac{\gamma L}{2v}\right)\cos\left(\frac{L\Delta}{v} + \varphi\right), \tag{17}$$

where A, B, C, D, and E are constants determined by the parameters of the experimental installation.

The effect of interference is described by the oscillating terms in these expressions, and reveals itself in the populations of both the 2S state (w_1), and the 2P state (w_2).

Finally, we ought to point to a circumstance important for understanding. The interference terms (oscillations of populations as functions of distance l) arise because each of the coefficients in the resultant superposition (16) is a sum of two phase-shifted terms proportional to $a_1(l)$ and $a_2(l)$. In other words, the interference is due to the fact that the resulting amplitude of a given state contains contributions from states that had previously been evolving along different 'paths'.

b) *The case of perpendicular* (*transverse*) *fields*

Assume that the fields E_1 and E_2 are orthogonal. We select the direction of field E_1 for the axis of quantization z, and the direction of field E_2 coincides with the x axis. In the polarizer (like in the previous case) there is a mixing of states for which the matrix elements of the d_z operator are nonzero. Given the same initial condition as before, the polarizer creates a superposition of the same states $|1\rangle$ and $|2\rangle$. Then at the entrance to System II the state of the atom is described by Eqn (14).

In the analyzer now we have a mixing of states for which the matrix elements of the d_z operator are nonzero. The double arrows in Fig. 13b indicate the allowed radiative transitions for the atom that enters the analyzer in the initial state (14). We see that the electric field E_2 in the analyzer (transverse to the field E_1) does not cause the additional coherent mixing of states $|1\rangle$ and $|2\rangle$, and there is no

interference. Indeed, the populations of states $|1\rangle$ and $|2\rangle$ are in this case

$$w_1 = \text{const}\,,$$
$$w_2 = A\exp\left(-\frac{\gamma L}{v}\right). \qquad (18)$$

Accordingly, the transverse field will only cause increased L_α background owing to the transitions indicated in Fig. 13b, but no interference.

Figure 14 shows the scheme of the double interferometer (a variant of the installation shown in Fig. 6) used in a series of experiments concerned with the interaction of an excited hydrogen atom with a metallic surface. All electrodes were made of sheet brass 0.08 cm thick, gold plated to about 5 microns, and placed in a vacuum chamber made from Armco iron.

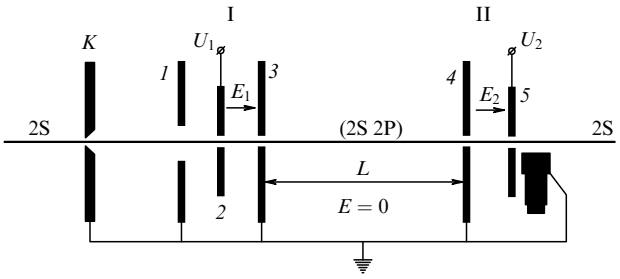

Figure. 14. Variant design of a double interferometer.

The widths in the slits were as follows: the collimator slit K — 0.005 cm, the slit in the guard electrode *1* of System I — 0.3 cm, all the rest (in electrodes *2* and *3* of System I, and electrodes *4* and *5* of System II) — 0.03 cm. The separations between electrodes *1*, *2*, and *3* of System I were 0.15 cm, and between electrodes *4* and *5* of System II — 0.2 cm. The distance L between Systems I and II could be varied from 0 to 2.5 cm.

In the preliminary experiment for a beam with energy of about 22 keV, consisting of H atoms with $F = 0$, we found that, in the absence of System II, the interference curve $I_{2P}(E_1)$ depicting the yield of 2P atoms as a function of the strength of the field between the electrodes *2* and *3* of System I, exhibits a clear maximum at $E_1 = 380$ V cm^{-1}. This superposition (2S – 2P) with the highest content of the 2P component was used in the subsequent measurements.

10.2 Experiment 1 — observation of radiative deexcitation of the 2P component

System II was removed, and with a constant longitudinal field $E_1 = 380$ V cm^{-1} the intensity of flux of 2P atoms as a function of the distance L between System I and the detector was measured — that is, we were observing the radiative deexcitation of the 2P component of the superposition (2S – 2P):

$$I_{2P} = I_0\exp\left(-\frac{\gamma L}{v}\right),$$

where v is the velocity of the atom, and $\gamma = 0.6265\times 10^8$ s^{-1}.

The observed dependence describes the curve of decay of the 2P component of the superposition (Fig. 15). It is a straight line

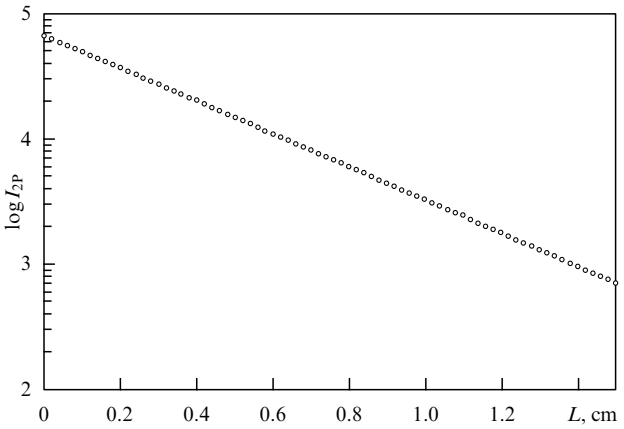

Figure 15. Decay curve of the 2P state.

$$\ln I_{2P}(L) = \text{const} - \frac{\gamma L}{v}\,,$$

whose slope allows the calculation of the velocity of atoms, as described earlier (see Section 7).

10.3 Experiment 2 — comparison of the 'slit' interaction with the effect of an external field

In this experiment we used the 'complete' scheme of the double interferometer — that is, both Systems I and II (see Fig. 14). For each value of L we made three measurements of the flux of 2P atoms: with $E_2 = \pm 15$ V cm^{-1}, and with shorted out and grounded plates *4* and *5*, i.e. for the case when E_2 is zero.

The experimental results are shown in Fig. 16. As ought to be expected, the oscillations of the flux of 2P atoms, caused by the longitudinal fields E_2 of the opposite sign, occur in counterphase (curves *a* and *b*). At the same time, a clear interference pattern is also observed in the absence of field E_2, when the electrodes *4* and *5* are shorted out and grounded (curve *c*), which can only be explained by the interaction between the atoms and the metallic slits. The magnitude of the effect (that is, the amplitude of the oscillations) corresponded to the longitudinal effective electric field E_{eff} acting on the atoms with a strength of the order of 10 – 12 V cm^{-1}.

Since the disturbance of the atom by System II is small, the perturbation theory can be used, and then the curve $I_{2P}(L)$ of

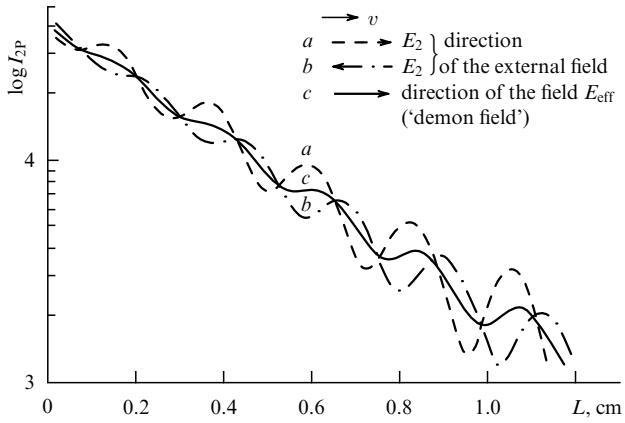

Figure 16. Comparative effects of different longitudinal fields.

yield of 2P atoms at $E_2 = 0$ will be described (in the former notation) by

$$I_{2P}(L) = A \exp\left(-\frac{\gamma L}{v}\right) + 2B \exp\left(-\frac{\gamma L}{2v}\right) \cos\left(\frac{\omega L}{v} + \varphi\right). \quad (19)$$

Disregarding the common factor of scale, we have $A = C_2/C_1$, where C_1 and C_2 are the amplitudes of the 2S and 2P states after interaction with System I. Coefficient B is the amplitude of mixing of the 2S and 2P states by System II, $\omega = 2\pi\nu$, and $\nu = 909.9$ MHz. Phase φ results from the action of both System I and System II.

As follows from formula (19), the period of spatial oscillations of the interference curve is $\Delta_L = v/\nu$, which at $v = 2.2 \times 10^8$ cm s^{-1} corresponds to 0.22 cm. This value is in good agreement with the curve shown in Fig. 16. From Eqn (19) it also follows that the experimental dependence $I_{2P}(L)$ is a sum of two curves: the mean line describing the exponential radiative deexcitation of the 2P state (the first term), and the superimposed oscillating structure, which is the interference curve of our concern. Accordingly, the latter can be obtained from the experimental curve $I_{2P}(L)$ by subtracting the exponential decay of the 2P state. Comparison of curve *c* with curves *a* and *b* (which not only have opposite phases, but different amplitudes of oscillations as well) revealed that the direction of the field E_{eff} coincides with that of the velocity of atoms [32].

For comparing the results of different experiments, it was necessary to evaluate the scale of the observed effect. For the scaling factor we used the ratio of the amplitude B of the interference curve to the coefficient A [the magnitude of $I_{2P}(L)$ measured at $L = 0$] expressed as a percentage.

Figure 17 gives a graphic summary of results obtained with different modifications of the interferometer.

10.4 Experiment 3 — the effect of the beam halo

The interferometer used in experiment 2 (see Fig. 16) was also employed for studying the possible effects of the beam halo. For this purpose, the entire assembly was tilted to an angle of approximately 30′ to the beam path (Fig. 18a). In this way, as the distance L increases, the beam will gradually approach one edge of the slit, and eventually touch it (Fig. 18b). Since about 98% of atoms in the beam are in the state 1S, the touch will increase the L_α background because these atoms will be excited to all possible states. The pitch of the background increase as L increases will depend on the size of the halo.

The parameters of the experiment were as follows: the energy of 2S atoms $E = 22$ keV, the beam thickness $\delta = 0.05$ mm, and the width of the slit $\Delta = 0.2$ mm. The outer atoms in the beam passed at a distance of $a = 0.075$ mm from the surface of the slit.

The beam touched the edge of the slit at $L = 10.8$ mm (Fig. 18c). The corresponding angle of tilt was $0.075/10.8 = 0.0069 = 23'$. With the distance changing in steps of $\Delta L = 0.2$ mm, the value of $L = 10.8$ mm corresponded to 54 experimental points. The 'immersion' of the slit edge into the beam on shifting by $\Delta L = 0.2$ mm is $0.75/54 = 0.0014$ mm $= 1.4$ μm, whence it follows that the halo is quite narrow and cannot have any considerable effect on what is observed.

10.5 Experiment 4 — direct proof of the long-range interaction of an excited atom with the metallic surface

It should be emphasized that the field E_{eff} just could not be eliminated and was a big nuisance in some experiments, and I

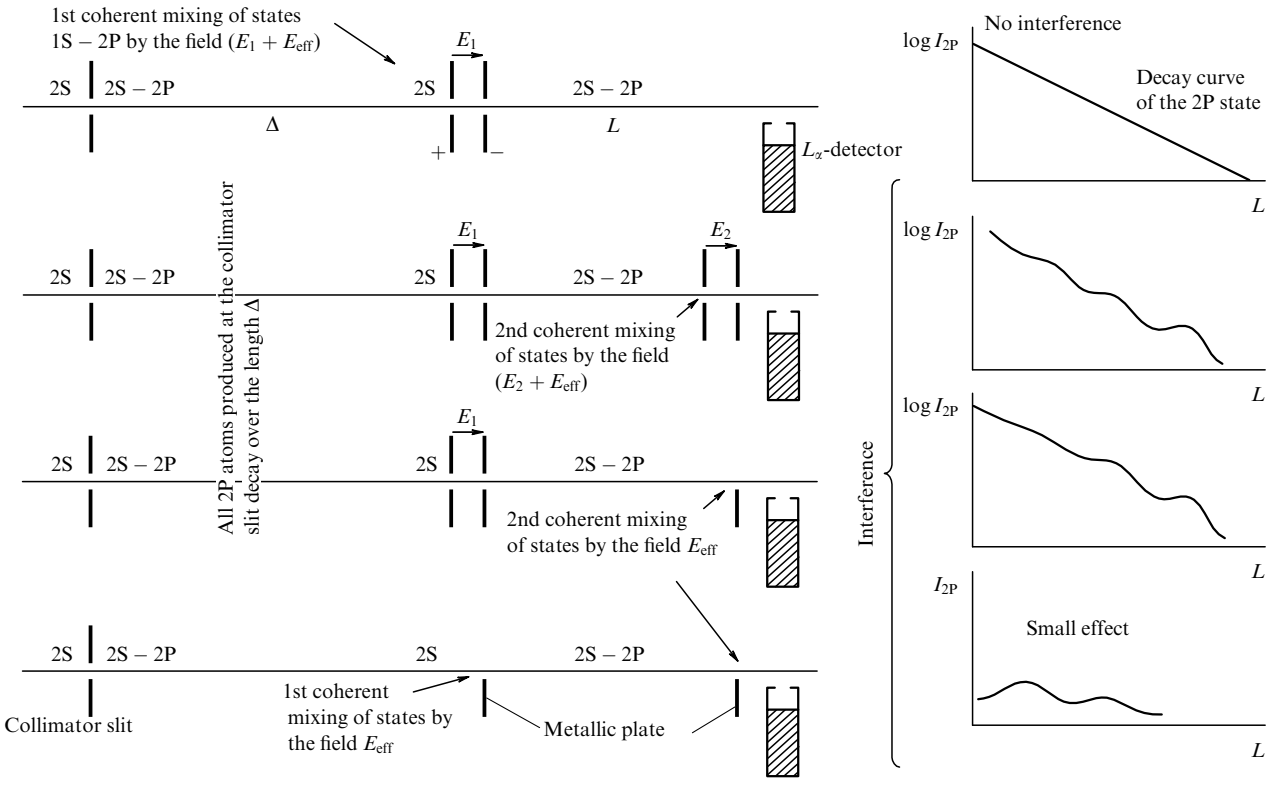

Figure 17. Summary of experimental results with different variants of the interferometer.

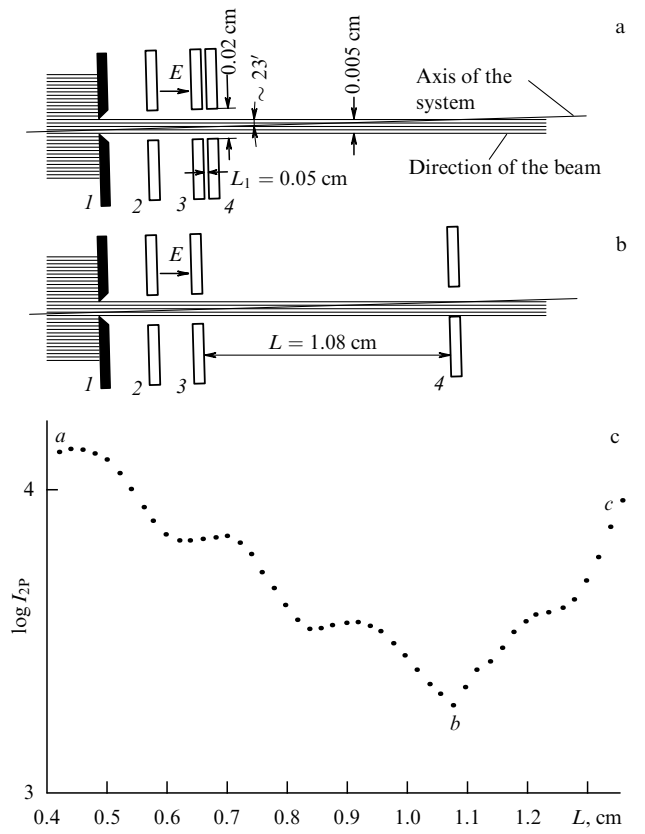

Figure 18. Schemes (a, b) and the results of experiments with a tilted interferometer.

must confess I was not a good Christian when I called it a 'demon field', a harassing artifact. It was only after a large number of experiments that I had to conclude that I was dealing with some kind of previously unknown long-range interaction of a moving excited hydrogen atom with a metallic surface. It is not so much the interaction itself which is stunning, but the immense (on the atomic scale) distance over which it occurs — up to 0.6–0.7 mm, or $\sim 10^7$ a.u.

A possible explanation of the production of the (2S–2P) superposition, when a 2S atom passes through a metallic slit, is based on the assumption that there are electric charges on the surface of the latter. In principle, such charges may be due to dielectric films, structural features of the metal surface, etc. It is hard to perceive, however, that these random charges would invariably produce a field of more or less the same magnitude and direction (in a slit 0.3 mm wide and the length of 6 mm along the beam path, for example). Nevertheless, the effect of random charges could not be disregarded.

At a particular stage of investigations during the discussion of the results obtained many of my opponents, without bothering to go into experimental details, argued that this phenomenon is due to the electric field produced by the above factors.

To refute such arguments, we performed the following experiment. In place of System II we used a single well-grounded slit formed by two strictly coplanar sharp edges made of gold-plated (~ 5 μm thick) hard brass. The edges were mounted on a flat base, so that their relative displacement along the beam path did not exceed 0.3 μm.

If for whatever reason the electric charges were induced on the surface of the edges, the resulting electric field could only be *transverse* — the geometry of the system is such that a *longitudinal* field is simply not feasible.

The layout of the experiment with this slit is shown in Fig. 19a, and the results in Fig. 19b. We see that when a superposition (2S–2P) passes through the slit, we observe a very clear interference pattern that can only be produced by a *longitudinal* field. The slits used in the experiments were from 0.2 to 1.2 mm wide; the curve shown in Fig. 19b (obtained with the 0.3 mm width) corresponds to the action of a *longitudinal* field of 12–15 V cm^{-1} on the beam.

If for any reason there were superficial electric charges on the edges, they could only produce the *transverse* electric field (Fig. 19c). In this case the effect observed could only be attributed to the combined action of the longitudinal components of E_1, E_2, E_3, and E_4, resulting from the curvature of the electric field. Observe that these components are directed in such a way that they cancel out in pairs.

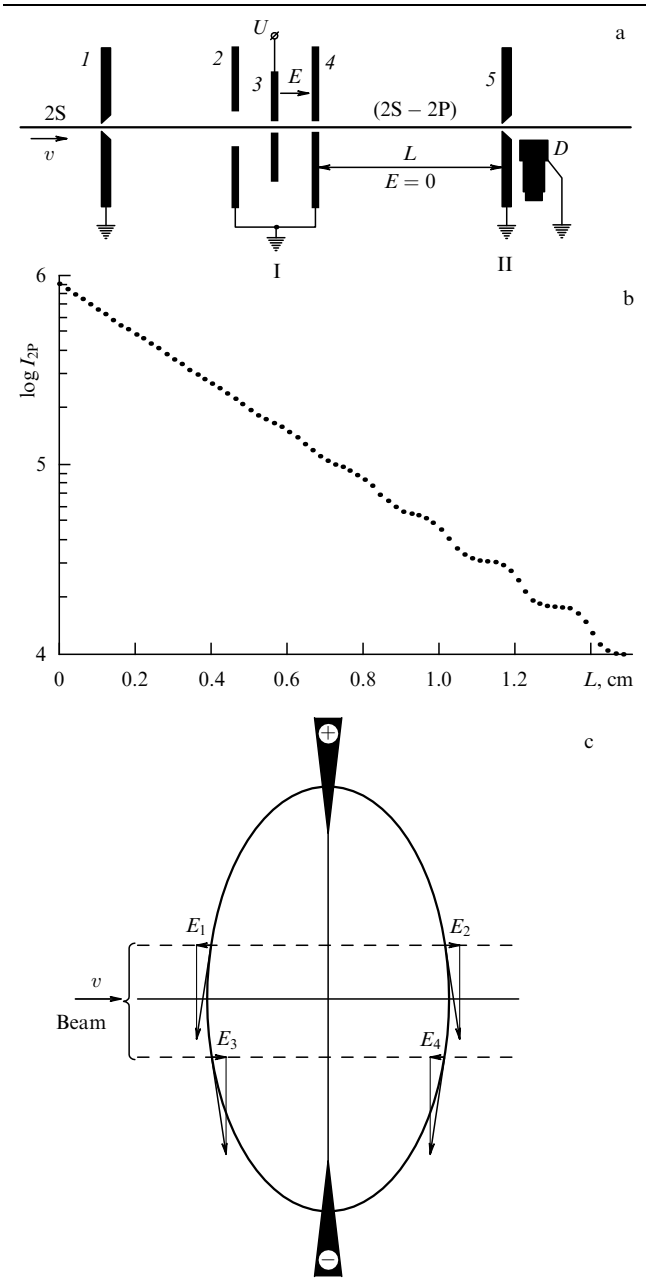

Figure 19. Schemes (a, c) and the results (b) of the experiment with a knife-edge slit.

Nevertheless, their effect is nonzero because of the decay of the 2P component over the length of action of the electric field.

Calculations indicate that the effect registered in the experiment could arise for a potential difference between the edges of about 12 V (then the strength of a transverse field in the gap would be 400 V cm^{-1}).

Obviously, the existence of such a potential difference would have completely distorted the interference pattern due to generation of the fields of unpredictable configuration between the edges and the grounded parts of the interferometer.

It is impossible to assume that a potential difference of 12 volts, of stable in time magnitude and polarity, would arise at random between two gilded edges screwed to a common equally gilded base. One must conclude therefore that there is no *longitudinal* field in the gap that could give rise to interference.

As it is, however, the interference is invariably observed in repeated experiments with gold coatings of varying thickness [33 – 35].

It is also important that the interference was clearly observed when one half of the slit was removed — that is, when the atoms passed over a sharp metallic edge. In such a geometry, the existence of a stable longitudinal field of the order of 10 V cm^{-1} near the surface, in addition to that always directed along the velocity of the atom, is contrary to all reasonable expectations.

From the arguments developed above we can only conclude that the interaction of an excited moving hydrogen atom with the metallic surface is of a nature yet unknown, and can only be phenomenologically attributed to the effective field $E_{\rm eff}$. This field, however, is not a conventional physical field, and cannot be registered with any macroscopic instrument.

As pointed out above, all attempts to explain the observed effect by the force interaction of the excited atom with a fluctuating electric field or with an image field in the metal failed, since the relevant contributions were orders of magnitude smaller that those observed.

The situation changed when B B Kadomtsev and M B Kadomtsev proposed an explanation of the effect based on the assumption that the atom flying over the metallic surface interacts with the conduction electrons in a thin surface layer. This results in an 'entangled state' of the atom with a huge number of conduction electrons, which are reflected by the surface back into the bulk, where their wave functions collapse over the mean free path. The collapses of the wave functions affect the correlation-coupled atom, which receives a coherent addition of the 2P state. The amount of this addition from each individual electron is infinitesimally small, but the net effect is observable because of the great number of electrons. Then, according to B B Kadomtsev, such an *irreversible* quantum effect is due to the coherent superposition of Einstein – Podolsky – Rosen (EPR) interactions, and ought to be considered in terms of correlations (like the Pauli principle) rather than in terms of forces [35 – 41].

Kadomtsev's hypothesis allows for a quantitative comparison between experimental results and theoretical predictions, thus verifying the theory. With this purpose we started a series of experiments concerned with studying how (and whether) the magnitude of the effect depends on the state of the conduction electrons in the metal.

Boris Borisovich Kadomtsev (1928 – 1998) had a knack rarely encountered in theoreticians: he had a fine feeling for the very essence of the experiment, and used to spend long hours in the laboratory appreciating the tiniest details. Watching enchanted the pen of the recorder as it plotted the next in turn interference curve, making comments, and drawing up plans for the future...

10.6 Experiment 5 — magnitude of the effect as a function of the distance between the atom and the metallic surface

This experiment was designed to verify the predicted (by the Kadomtsev theory) dependence of the amplitude of the (2S – 2P) transition — that is, the scale of the effect — on the distance l between the atoms of the beam and the metallic surface. We used the configuration shown in Fig. 19, with a

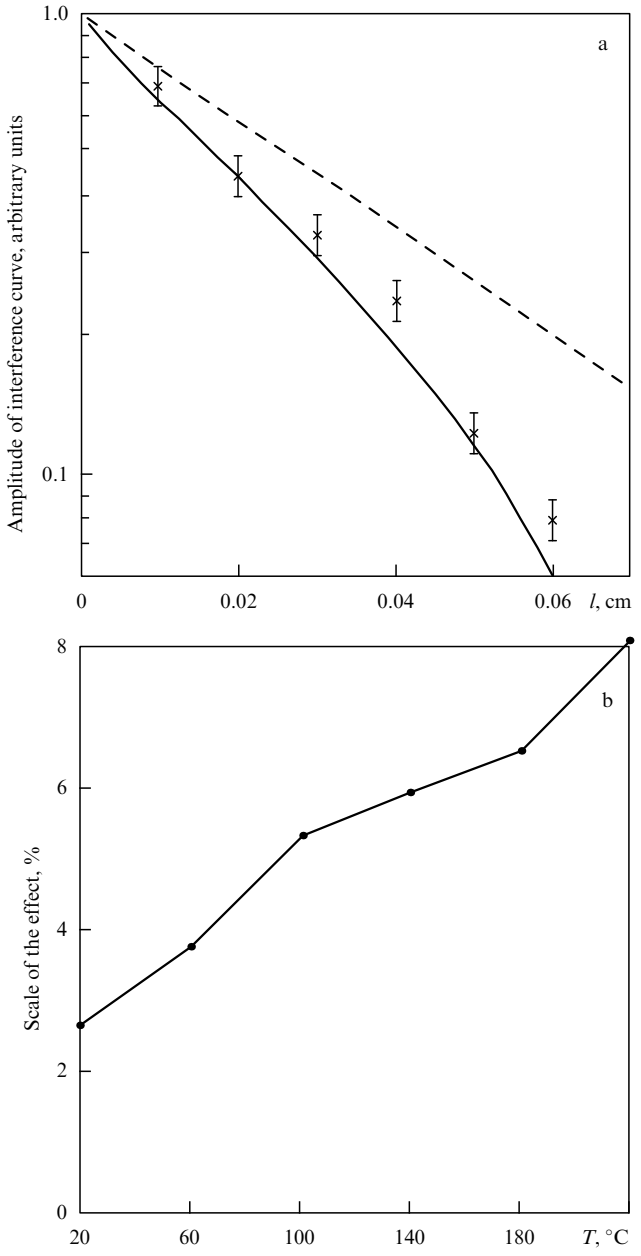

Figure 20. Scale of the effect vs. the distance l between the atom and metallic surface (a), and vs. the temperature of the metal (b).

slit of variable width, formed by rectangular plates with a thickness of $D = 0.7$ mm.

The results are displayed in Fig. 20a. The theoretical dependence shown by the solid line corresponds to a slit with a thickness of $D = 0.7$ mm. The dotted line corresponds to $D = 0$ — that is, with the slit formed by sharp edges (then the function $I_{2P}(l)$ becomes exponential and simply reduces to $\exp(-2\pi l/\Lambda_L)$, where $\Lambda_L = v/\nu$). The 'Lamb wavelength' Λ_L, i.e. the period of spatial oscillations of the interference curve, is huge on the atomic scale, and does not involve any characteristic of the metallic surface. Hence it follows that the observed effect is indeed a long-range interaction, and is a universal phenomenon [32].

10.7 Experiment 6 — the effect of the slit wall perpendicular to the beam path

Kadomtsev's theory allows the contributions of individual elements of the slit to the total effect to be evaluated — namely, the contribution of the wall perpendicular to the beam, and the wall parallel to the beam, above which the atoms are flying.

In this experiment we compared the magnitude of the effect caused by the knife-edge slit, and a slit of the same width (0.3 mm) formed by two parallel gold wires 15 microns thick, which corresponded to the width of the butt of the knife-edge slit (in both cases the flight time was 7.5×10^{-11} s).

The result was as follows: the magnitude of the effect for the wire slit was about an order of magnitude smaller than that for the knife-edge slot, in complete agreement with the theoretical prediction.

Experiments concerning the effects of the wall extending along the beam are yet to be performed.

10.8 Experiment 7 — magnitude of the effect versus the temperature of the metal

This experiment was designed to study the scale of the effect as a function of the temperature of the metal. We used a gold-plated strip of soft iron measuring 3×0.2 mm, with a cut-out slit 0.25 mm wide. The strip was heated with alternating current; the temperature range that did not lead to misalignment of the interferometer was not too broad — from 25 to 250 °C. The results of this experiment are shown in Fig. 20b.

The measurements indicated that as the temperature increases, there is a sharp increase in the useful signal along with the increase in the background (which is quite natural). We see that a relatively small temperature increase (by about 200 °C) leads to a considerable enhancement in the coherent mixing of 2S and 2P states.

The strong influence of the temperature of the metal on the magnitude of the effect is likely to be explained by the increasing number of EPR pairs as the atom interacts with the conduction electrons, whose state in the thin surface layer must be altered. This conclusion, however, needs a thorough experimental verification.

10.9 Experiment 8 — magnitude of the effect versus the crystal structure of the metal

Like the previous one, this experiment is also concerned with studying the dependence of the magnitude of the effect on the state of electrons in the metal. In this series we used slits formed with massive plates of gold – silver alloy (92% Au + 8% Ag) and pure palladium. These metals have similar values of the work function, but substantially different Fermi surfaces. The microstructure of the plates varied considerably: highly cold-hardened samples (this is the reason why we used the alloy rather than the highly moldable pure gold), and samples annealed at the recrystallization temperature. In other words, we had either coarse-grained or fine-grained metal slits.

The preparation was as follows: the chunks of metal were repeatedly rolled out with rollers to a thickness of 0.5 mm, the halves of the slits were made, polished by conventional methods, treated for about 10 s in a mixture of nitrous and hydrochloric acids, rinsed with distilled water, dried with alcohol and installed in the interferometer.

After taking the interference curves, the samples were quickly heated to the recrystallization temperature and cooled by dipping into distilled water. Then they were once again washed with acid, water and alcohol. The slit was placed back into the interferometer with great care, so that the initial gap of 0.3 mm would change by no more than 0.01 mm.

The results of this experiment are as follows. For cold-hardened gold the magnitude of the effect reduced to about 0.3% (for electrodeposited coatings it varied within 2 – 4%); for palladium, the effect was somewhat greater, as large as 1.70%. It ought to be noted that such comparison makes little sense, since the degree of cold-hardening for the two samples was undetermined.

After annealing, the scale of the effect for both metals changed considerably: it was 2.3% for gold + silver, and 7.25% for palladium. Figure 21 shows the interference curves for the cold-hardened ($B/A = 1.70\,\%$) and annealed ($B/A = 7.25\,\%$) palladium.

It is highly likely that the last three experiments point to the strong dependence of the observed effect on the state of the conduction electrons: the magnitude of the effect varies severalfold (recall that the Kadomtsev theory is based on the assumption that the atom interacts with the quasi-free electrons in the thin surface layer). At the same time, it is hard to see which of the characteristics of the metal (or, more precisely, the state of the metallic surface) could exhibit such a degree of variation. The study of this extremely sophisticated

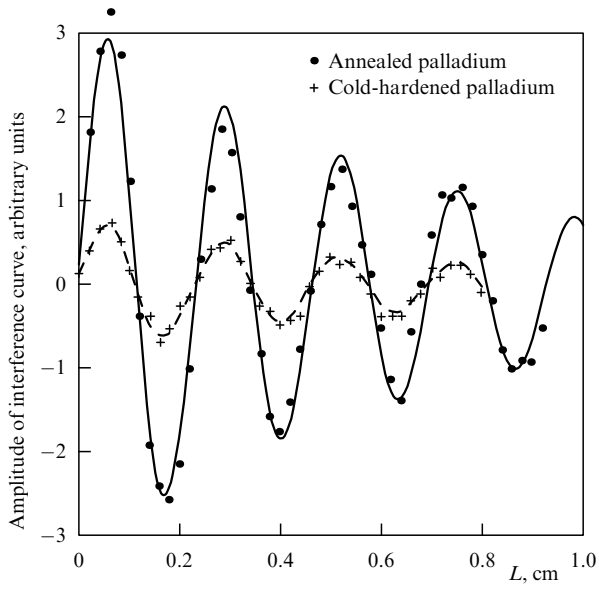

Figure 21. Comparison of the scales of effect for cold-hardened (+) and annealed (•) palladium.

problem is beyond our capabilities — then we would digress into the domain of the physics of surface phenomena and solid-state physics. Because of this, our plans in this direction are only concerned with improved experiments on the effects of the temperature, with the purpose of extending the temperature range.

Much more 'transparent', and perhaps much more principally important, seem the experiments concerned with the dependence of the scale of the effect on the velocity of atoms.

The system shown in Fig. 19a was used for observing the total effect caused by both System I that creates the superposition (2S – 2P) and System II (i.e. metallic slit) that causes additional mixing of 2S and 2P states. Therefore, in order to distinguish the effect of this slit alone as a function of the velocity of atoms, we must eliminate the contribution of System I (also depending on the atomic velocity) at the stage of data processing.

These experiments were not yet complete at the time of writing this review, since a considerable modification of our installation was required in order to be able to vary the speed (that is, the energy) of the atoms within sufficiently broad limits.

11. Conclusions

The studies described in this paper relate to the science that could be aptly called the 'optics of atomic states'. The measurements of characteristics of these states using atomic interferometers opens new possibilities for validation of quantum electrodynamics at low energies, since this method provides for precision measurements of δ for hydrogen and deuterium atoms, and for some hydrogen-like ions as well [37], for measurements of frequencies of fine- and hyperfine-structure splitting of levels, for measuring the electrical radius of the proton, the radius of alpha-particle, etc. [43].

Our measurement of δ for the hydrogen atom is the only study where a high-precision measurement of the Lamb shift was performed with a purely interference technique rather than with common radiospectroscopy. Not to mention the general metrological importance of the availability of an alternative measurement technique, the interference method has a principal advantage: it does not introduce any disturbing field. Because of this, the accuracy of the measurement is much higher (about 10^{-5} of the linewidth of fine-structure splitting).

Apart from its metrological importance, the observation of interference of atomic states is of interest by itself. This is because the interference pattern developed over a broad range of phase shifts is extremely sensitive to the parameters of the interfering states, which may be manifested in previously unknown aspects. An example is the discovery of the long-range interaction of the excited hydrogen atom with a metallic surface, made while measuring the Lamb shift. An explanation of the nature of this interaction, regarded as an *irreversible* quantum effect, was proposed by B B Kadomtsev. His theoretical construction goes far beyond the limits of today's concepts about the interaction of an excited atom with a metallic surface, and therefore calls for careful experimental verification.

Just these studies, which are of fundamental and profound importance, will be continued in further experiments, in which, to our grief, Boris Borisovich Kadomtsev will take part no longer.

The author is deeply grateful to B B Kadomtsev, V P Yakovlev, G F Bassani, M B Kadomtsev, V G Pal'chikov, and Yu A Kucheryaev for discussions and invariable assistance.

12. Appendices

Appendix I

A hydrogen atom passes with velocity v through the electric field of the interferometer. In the atomic frame of reference, the atom is under the action of variable field $\vec{\mathcal{E}}(t)$. If the atom travels along the field, then in the atomic rest frame there is no magnetic field, and the electric field does not change. The direction of movement of the atom (and the direction of $\vec{\mathcal{E}}$) coincides with the z axis.

The electric field induces transitions between 2S and 2P states. Let us consider the simplest case when the hyperfine-structure splitting of levels is disregarded, as are the transitions between the states $2S_{1/2}$ and $2P_{3/2}$, which is justified for 'normal' fields. In such a statement, the problem is reduced to the analysis of the behavior of the two-level system $2S_{1/2}-2P_{1/2}$ in the external variable electric field.

The Schrödinger equation for the wave function of the atom $\Psi(\bar{r}, t)$ is

$$\mathrm{i}\hbar\frac{\partial\Psi}{\partial t} = \left[\mathrm{H}_0 + \hat{V}(t)\right]\Psi\,. \tag{I.1}$$

Here H_0 is the Hamiltonian of the free atom, and $\hat{V}(t)$ is the interaction with the electric field

$$\hat{V}(t) = -\hat{\mathrm{d}}\vec{\mathcal{E}}(t) = -\hat{\mathrm{d}}_z\mathcal{E}(t) = -\hat{\mathrm{d}}_z\mathcal{E}_0F(t)\,, \tag{I.2}$$

where $\hat{\mathrm{d}}_z$ is the operator of z component of the dipole moment, $\mathcal{E}_0$ is the amplitude of the field, and the function $F(t)$ describes the profile of field variation.

The solution of the Schrödinger equation is sought in the form

$$\Psi(\bar{r}, t) = b_1(t)\psi_1(\bar{r}) + b_2(t)\psi_2(\bar{r})\,, \tag{I.3}$$

where ψ_1 and ψ_2 are the eigenfunctions of H_0 that describe the states $2S_{1/2}$ and $2P_{1/2}$, respectively.

Functions $b_1(t)$ and $b_2(t)$, which are the amplitudes of probabilities of finding the system in the states $2S_{1/2}$ and $2P_{1/2}$, satisfy the set of equations

$$\mathrm{i}\hbar\frac{\mathrm{d}b_n}{\mathrm{d}t} = E_nb_n + \sum_m b_m\langle\psi_n|\hat{V}|\psi_m\rangle\,. \tag{I.4}$$

The matrix elements are

$$\langle\psi_1|\hat{V}(t)|\psi_2\rangle = \langle\psi_2|\hat{V}(t)|\psi_1\rangle \equiv \mathrm{d}\mathcal{E}_0F(t)\,,$$

where $\mathrm{d} = \int_{2S_{1/2}}(\bar{r})ez\,\psi_{2P_{1/2}}(\mathcal{E})\,\mathrm{d}V = \sqrt{3}ea_0$ (a_0 is the Bohr radius). The energy E_2 has the imaginary part equal to $-\mathrm{i}\hbar/(2\tau)$ (τ is the lifetime of a hydrogen atom in the state 2P).

Now it is convenient to go over to the functions φ_1 and φ_2:

$$b_1 = \varphi_1\exp\left(-\mathrm{i}\frac{E_1}{\hbar}t\right), \quad b_2 = \varphi_2\exp\left(-\frac{E_2}{\hbar}t\right),$$

$$\left(|\varphi_1|^2 = |b_1|^2 \text{ и } |\varphi_2|^2 = |b_2|^2\right) \tag{I.5}$$

and the new variable $z = vt$.

Functions $\varphi_1(z)$, $\varphi_2(z)$ satisfy the set of equations

$$\mathrm{i}\frac{\mathrm{d}\varphi_1}{\mathrm{d}z} = qF(z)\varphi_2\,, \quad \mathrm{i}\frac{\mathrm{d}\varphi_2}{\mathrm{d}z} = P\varphi_2 + qF(z)\varphi_1\,, \tag{I.6}$$

where $q = \mathrm{d}\mathcal{E}_0/(\hbar v)$, $p = 2\pi\delta/v$, and $P = (E_2 - E_1)/(\hbar v) = p - 1/(2\tau v)$.

Assume that the profile of field $\mathcal{E}$ is rectangular (dropping suddenly at the ends), and the observation point is located at a distance L from the rear end of the field.

Let us find the quantity $|\varphi_2|^2$ at the observation point given that at $z = 0$ we have $\varphi_1(0) = 1$ and $\varphi_2(0) = 0$.

The solution in the interval $0 < z < l$ takes the form

$$\varphi_1(z) = c_1\exp(-\mathrm{i}\Lambda_1 z) + c_2\exp(-\mathrm{i}\Lambda_2 z)\,,$$
$$\varphi_2(z) = q\left[\frac{c_1}{\Lambda_1 - P}\exp(-\mathrm{i}\Lambda_1 z) + \frac{c_2}{\Lambda_2 - P}\exp(-\mathrm{i}\Lambda_2 z)\right], \tag{I.7}$$

where $\Lambda_{1,2}$ are the roots of equation $\Lambda(\Lambda - P) = q^2$, i.e.

$$\Lambda_{1,2} = \frac{P}{2} \pm \sqrt{\frac{1}{4}P^2 + q^2}\,. \tag{I.8}$$

The condition of sewing together at the point $z = 0\,[\varphi_1(0) = 1\,,\ \varphi_2(0) = 0]$ gives

$$c_1 = \frac{\Lambda_1 - P}{\Lambda_1 - \Lambda_2}\,, \quad c_2 = \frac{\Lambda_2 - P}{\Lambda_2 - \Lambda_1}\,.$$

For $z > l$ (with regard to sewing together at point $z = l$) we have

$$\varphi_2(z) = \varphi_2(l)\exp\left[-\mathrm{i}P(z - l)\right]. \tag{I.9}$$

Thus, the sought-for quantity φ_2 at the observation point $z = l + L$ is given by

$$\varphi_2 = \exp(-\mathrm{i}PL)\frac{q}{\Lambda_1 - \Lambda_2}\left[\exp(-i\Lambda_1 l) - \exp(-\mathrm{i}\Lambda_2 l)\right]. \tag{I.10}$$

Then

$$|\varphi_2|^2 = \exp\left(-\frac{L}{l_0}\right)\frac{2q^2\exp[-l/(2l_0)]}{(\Lambda_1 - \Lambda_2)^2 + (\mu_1 - \mu_2)^2}$$
$$\times\left[\cosh(\mu_1 - \mu_2)l - \cos(\Lambda_1 - \Lambda_2)l\right], \tag{I.11}$$

where $l_0 = v\tau$.

Calculating the real and imaginary parts of the roots $\Lambda_{1,2}$, we get

$$\Lambda_1 - \Lambda_2 = \sqrt{\frac{1}{2}\left(\sqrt{a^2 + b^2} + a\right)}\,,$$

$$\mu_1 - \mu_2 = -\sqrt{\frac{1}{2}\left(\sqrt{a^2 + b^2} - a\right)}\,,$$

where

$$a = p^2 + 4q^2 - \frac{1}{4l_0^2}\,, \quad b = \frac{p}{l_0}\,.$$

If $b/a \ll 1$, then $\Lambda_1 - \Lambda_2 \cong \sqrt{a}$, and $\mu_1 - \mu_2 \cong -b/(2\sqrt{a})$.

Now we introduce the notation

$$x = \frac{2q}{P} = \frac{\mathrm{d}\mathcal{E}_0}{\pi\hbar\delta}\,,$$

$$l_0 = v\tau = \frac{l}{T\gamma}\,, \quad \text{where} \quad T \quad \text{is the flight time, and}$$

$$K = \frac{1}{2}\exp\left(-\frac{L}{l_0}\right) \text{ (constant coefficient)}\,.$$

Then the probability of yield of the 2P state can be finally represented as

$$|\varphi_2|^2 = K\frac{x^2}{1 + x^2}\left[\cosh\frac{\tau T}{2\sqrt{1 + x^2}} - \cos 2\pi\delta T\sqrt{1 + x^2}\right]$$
$$\times\exp\left(-\frac{\gamma T}{2}\right). \tag{I.12}$$

(This equation was derived by V P Yakovlev.)

Appendix II

To evaluate the magnitude of L_α background produced by the cascade radiative deexcitation of highly excited hydrogen atoms, let us find the number of such atoms that transit to level 2P from the states with $3 \leqslant n \leqslant 25$.

We shall also estimate the number of atoms that go to the level $2S_{1/2}$, in order to find out how this process affects the intensity of the 2S component of the beam.

The following initial assumptions are made:

(1) We estimate the number of H_{2P} and H_{2S} atoms that form on the trajectory segment $\Delta x = x_2 - x_1 = 1$ cm after travelling the distance of 200 cm from the exit slit of the charge-exchange chamber ($x_2 = 201$ cm, $x_1 = 200$ cm);

(2) Only the dipole transitions are taken into account, when $\Delta l = 1$. Then

(a) the transitions to level 2P occur from all nS and nD states ($3 \leqslant n \leqslant 25$);

(b) the transitions to level 2S occur from all nP states with $3 \leqslant n \leqslant 25$.

The number of atoms in the state i that remain by the time $t_1 = x_1/v$ is

$$N_{i1} = N_{i0}\exp(-\mathfrak{W}t_1)\,,$$

and by the time $t_2 = x_2/v$ one finds

$$N_{i2} = N_{i0}\exp(-\mathfrak{W}t_2)\,,$$

where N_{i0} is the number of atoms of type i that were available at the time $t = 0$ (we assume that $N_i \sim 1/n^3$), and $\mathfrak{W}$ is the probability of the appropriate radiative transition.

The number of atoms that undergo the transition on the leg of a trajectory from x_1 to x_2 (that is, over the time $\Delta t = t_1 - t_2$) is given by

$$\Delta N_i = N_{i2} - N_{i1} = N_{i0}\left[\exp(-\mathfrak{W}t_1) - \exp(-\mathfrak{W}t_2)\right]. \tag{II.13}$$

In the case under consideration, when the velocity of atoms is $v = 2\times10^8$ cm s^{-1}, we have

$$t_1 = \frac{200}{2\times10^8} = 1.00000\times10^{-6}\ \mathrm{s}\,,$$

$$t_2 = \frac{201}{2\times10^8} = 1.00500\times10^{-6}\ \mathrm{s}\,.$$

The probabilities of the transitions of interest we denote by

I $(n\mathrm{S} \to 2\mathrm{P})$ ω_n,
II $(n\mathrm{D} \to 2\mathrm{P})$ A_n,
III $(n_\mathrm{P} \to 2\mathrm{S})$ B_n.

The proportions of atoms that go into 2S and 2P levels under the specified conditions are

$$K_\mathrm{I} = \sum_{n=3}^{25} \frac{1}{n^3}\left[\exp(-\omega_n t_1) - \exp(-\omega_n t_2)\right],$$

$$K_\mathrm{II} = \sum_{n=3}^{25} \frac{1}{n^3}\left[\exp(-A_n t_1) - \exp(-A_n t_2)\right],$$

$$K_\mathrm{III} = \sum_{n=3}^{25} \frac{1}{n^3}\left[\exp(-B_n t_1) - \exp(-B_b t_2)\right].$$

In Tables 1–3 we have listed the contributions of individual nS and nD levels in the course of transitions to the level 2P, and those of nP levels to the level 2S — that is, the values of

$$\mathrm{S}_n = \frac{1}{n^3}\left[\exp(-\omega_n t_1) - \exp(-\omega_n t_2)\right],$$

$$\mathrm{D}_n = \frac{1}{n^3}\left[\exp(-A_n t_1) - \exp(-A_n t_2)\right],$$

$$\mathrm{P}_n = \frac{1}{n^3}\left[\exp(-B_n t_1) - \exp(-B_n t_2)\right],$$

Table 1. Transition $n\mathrm{S} \to 2\mathrm{P}$, $x_1 = 200$ cm, $t_1 = 1.0000 \times 10^{-6}$ s.

n	S_n	n	S_n	n	S_n
3	2.085531×10^{-6}	11	3.711682×10^{-7}	19	1.597899×10^{-8}
4	1.519367×10^{-5}	12	2.366875×10^{-7}	20	1.177959×10^{-8}
5	1.416291×10^{-5}	13	1.490647×10^{-7}	21	8.810538×10^{-9}
6	8.143157×10^{-6}	14	9.681163×10^{-8}	22	6.677419×10^{-9}
7	4.221422×10^{-6}	15	6.461963×10^{-8}	23	5.122240×10^{-9}
8	2.195807×10^{-6}	16	4.419727×10^{-8}	24	3.973122×10^{-9}
9	1.182557×10^{-6}	17	3.089548×10^{-8}	25	3.162617×10^{-9}
10	6.643010×10^{-7}	18	2.202388×10^{-8}		

$K_\mathrm{I} \sum_3^{25} \mathrm{S}_n = 4.892033 \times 10^{-5}$ $\qquad$ $K'_\mathrm{I} = \sum_3^6 \mathrm{S}_n = 3.058527 \times 10^{-5}$

Table 2. Transition $n\mathrm{D} \to 2\mathrm{P}$, $x_1 = 200$ cm, $t_1 = 1.0000 \times 10^{-6}$ s.

n	D_n	n	D_n	n	D_n
3	8.585597×10^{-31}	11	1.334235×10^{-6}	19	9.122887×10^{-8}
4	1.690584×10^{-12}	12	9.415839×10^{-7}	20	6.839272×10^{-8}
5	2.971152×10^{-8}	13	6.585476×10^{-7}	21	5.772595×10^{-8}
6	6.854659×10^{-7}	14	4.615734×10^{-7}	22	3.974878×10^{-8}
7	1.975003×10^{-6}	15	3.260777×10^{-7}	23	3.077777×10^{-8}
8	2.561119×10^{-6}	16	2.328492×10^{-7}	24	2.406058×10^{-8}
9	2.345664×10^{-6}	17	1.682884×10^{-7}	25	1.897925×10^{-8}
10	1.834151×10^{-6}	18	1.231470×10^{-7}		

$K_\mathrm{II} = \sum_3^{25} \mathrm{D}_n = 1.395061 \times 10^{-5}$, $\qquad$ $K'_\mathrm{II} = \sum_3^6 \mathrm{D}_n = 7.151828 \times 10^{-7}$

Table 3. Transition $n\mathrm{S} \to 2\mathrm{P}$, $x_1 = 1000$ cm, $t_1 = 5.0000 \times 10^{-6}$ s.

n	S_n	n	S_n	n	S_n
3	1.169000×10^{-9}	11	2.442327×10^{-7}	19	1.460848×10^{-8}
4	5.048924×10^{-8}	12	1.654780×10^{-7}	20	1.090818×10^{-8}
5	8.179064×10^{-8}	13	1.125345×10^{-7}	21	8.244763×10^{-9}
6	4.305664×10^{-7}	14	7.731798×10^{-8}	22	6.3022976×10^{-9}
7	6.741261×10^{-7}	15	5.383228×10^{-8}	23	4.870020×10^{-9}
8	6.472579×10^{-7}	16	3.802616×10^{-8}	24	3.800458×10^{-9}
9	5.032542×10^{-7}	17	2.725681×10^{-8}	25	2.993439×10^{-9}
10	3.570264×10^{-7}	18	1.981856×10^{-8}		

$K_\mathrm{I} = \sum_3^{25} \mathrm{S}_n = 3.485920 \times 10^{-6}$, $\qquad$ $K'_\mathrm{I} = \sum_3^6 \mathrm{S}_n = 5.128620 \times 10^{-7}$

as well as the values of

$$K_\mathrm{I} = \sum_3^{25} \mathrm{S}_n, \quad K_\mathrm{II} = \sum_3^{25} \mathrm{D}_n, \quad K_\mathrm{III} = \sum_3^{25} \mathrm{P}_n$$

and

$$K'_\mathrm{I} = \sum_3^{6} \mathrm{S}_n, \quad K'_\mathrm{II} = \sum_3^{6} \mathrm{D}_n, \quad K'_\mathrm{III} = \sum_3^{6} \mathrm{P}_n.$$

According to Ref. [44], the distribution of hydrogen atoms with respect to S, P and D states after charge exchange of protons with an energy of $E \sim 20$ keV in molecular hydrogen is

$\mathrm{S} \sim 30\,\%$,
$\mathrm{P} \sim 55\,\%$,
$\mathrm{D} \sim 15\,\%$.

Accordingly, the total share of H atoms with $3 \leqslant n \leqslant 25$ that go to 2P and 2S levels on the path leg $\Delta x = 201 - 200 = 1$ cm is equal to

$$K_{2\mathrm{P}} = 0.3K_\mathrm{I} + 0.15K_\mathrm{II} = 1.68 \times 10^{-5},$$

$$K_{2\mathrm{S}} = 0.55K_\mathrm{III} = 1.13 \times 10^{-5}.$$

Since the lifetime of $\mathrm{H}_{2\mathrm{P}}$ is $\tau_{2\mathrm{P}} = 1.596 \times 10^{-9}$ s, we must conclude that at $v = 2 \times 10^8$ cm s^{-1} over the length $\Delta x = 1$ cm about 95% of the $\mathrm{H}_{2\mathrm{P}}$ formed will decay. Then, if the flow rate of $\mathrm{H}_{1\mathrm{S}}$ atoms is 10^{11} s^{-1}, the number of L_α quanta emitted by one centimeter of the beam over the area $x \sim 200$ cm is about 10^6 quanta per second.

This estimate is in sufficiently good agreement with the experiment.

From Tables 1 and 2, and from comparison of K_I with K'_I and K_II with K'_II, we deduce that the main contribution to the background component in question comes from the levels 4S and 5S, which are well populated and have relatively long lifetimes with respect to $4\mathrm{S} \to 2\mathrm{P}$ and $5\mathrm{S} \to 2\mathrm{P}$ transitions ($\tau_{4\mathrm{S}-2\mathrm{P}} = 3.879 \times 10^{-7}$ s, $\tau_{5\mathrm{S}-2\mathrm{P}} = 7.761 \times 10^{-7}$ s). Since these states cannot be ionized by a field with strength 550,000 V cm^{-1}, there is little sense in using a high-voltage gap as a filter reducing the background. With a flight length of about 10 meters, however, such a filter will produce a noticeable effect, as follows from Table 3 where the sums $K_\mathrm{I} = \sum_3^{25} \mathrm{S}_n$ and $K'_\mathrm{I} = \sum_3^6 \mathrm{S}_n$ are calculated for $x_1 = 1000$ cm.

In Table 4 we list similar estimates for the transition $n\mathrm{P} \to 1\mathrm{S}$ — that is, for the lines in the Lyman series starting with L_β. The short-wave background component makes up about one-seventh of the total background created by the $n\mathrm{S} \to 2\mathrm{P}$ and $n\mathrm{D} \to 2\mathrm{P}$ transitions discussed above. If necessary, this component can easily be removed with a LiF filter or by introducing a high-voltage gap ($K'_{\mathrm{IV}} = 1.177 \times 10^{-12}$).

Table 4. Transition $n\mathrm{P} \to 1\mathrm{S}$, $x_1 = 200$ cm, $t_1 = 1.0000 \times 10^{-6}$ s.

n	P_n	n	P_n	n	P_n
3	4.885583×10^{-75}	11	4.998075×10^{-7}	19	2.413787×10^{-7}
4	1.104181×10^{-32}	12	6.147032×10^{-7}	20	1.936138×10^{-7}
5	1.490336×10^{-18}	13	6.402618×10^{-7}	21	1.551698×10^{-7}
6	1.177308×10^{-12}	14	6.015138×10^{-7}	22	1.245092×10^{-7}
7	7.481180×10^{-10}	15	5.296655×10^{-7}	23	1.001650×10^{-7}
8	2.054048×10^{-8}	16	4.478001×10^{-7}	24	8.086217×10^{-8}
9	1.202381×10^{-7}	17	3.691563×10^{-7}	25	6.554565×10^{-8}
10	3.091751×10^{-7}	18	2.997615×10^{-7}		

$$K_{\mathrm{IV}} = \sum_3^{25} \mathrm{P}_n = 5.414617 \times 10^{-6}\,, \qquad K'_{\mathrm{IV}} = \sum_3^{6} \mathrm{P}_n = 1.177308 \times 10^{-12}$$

The value of the coefficient $K_{\mathrm{III}} = 2.059 \times 10^{-5}$ (Table 5), which characterizes the intensity of transitions to the 2S level, indicates that the above processes have virtually no effect on the current of $\mathrm{H}_{2\mathrm{S}}$ atoms.

Table 5. Transition $n\mathrm{P} \to 2\mathrm{S}$, $x_1 = 200$ cm, $t_1 = 1.0000 \times 10^{-6}$ s.

n	P_n	n	P_n	n	P_n
3	7.014248×10^{-13}	11	1.091672×10^{-6}	19	5.959798×10^{-8}
4	4.667582×10^{-8}	12	7.201508×10^{-7}	20	4.437014×10^{-8}
5	1.387465×10^{-6}	13	4.806024×10^{-7}	21	3.345567×10^{-8}
6	3.768924×10^{-6}	14	3.257221×10^{-7}	22	2.552574×10^{-8}
7	4.323480×10^{-6}	15	2.224933×10^{-7}	23	1.969038×10^{-8}
8	3.517573×10^{-6}	16	1.573634×10^{-7}	24	1.534486×10^{-8}
9	2.483750×10^{-6}	17	1.121301×10^{-7}	25	1.207252×10^{-8}
10	1.659624×10^{-6}	18	8.115237×10^{-8}		

$$K_{\mathrm{III}} = \sum_3^{25} \mathrm{P}_n = 2.059083 \times 10^{-5}\,, \qquad K'_{\mathrm{III}} = \sum_3^{6} \mathrm{P}_n = 5.203066 \times 10^{-6}$$

References

1. Zel'dovich Ya B *Zh. Eksp. Teor. Fiz.* **36** 964 (1959) [*Sov. Phys. JETP* **9** 682 (1959)]
2. Weinberg S "Nobel Lecture, December 8, 1979" *Usp. Fiz. Nauk* **132** 201 (1980)
3. Glashow Sh L "Nobel Lecture, December 8, 1979" *Usp. Fiz. Nauk* **132** 219 (1980)
4. Salam A "Nobel Lecture, December 8, 1979" *Usp. Fiz. Nauk* **132** 229 (1980)
5. Okun' L B *Leptony i Kvarki* (Leptons and Quarks) 2nd ed (Moscow: Nauka, 1990) [Translated into English (Amsterdam: North Holland, 1984)]
6. Khriplovich I B *Nesokhranenie Chetnosti v Atomnykh Yavleniyakh* (Violation of Parity in Atomic Phenomena) (Moscow: Nauka, 1981)
7. Miniatura Ch et al. *Appl. Phys. B* **54** 347 (1992)
8. Robert J et al. *Europhys. Lett.* **16** (1) 29 (1991)
9. Chaĭka M P *Interferentsiya Vyrozhdennykh Atomnykh Sostoyaniĭ* (Interference of Degenerate Atomic States) (Leningrad: Izd. LGU, 1975)
10. Novikov L N, Skrotskiĭ G V, Solomakho G I *Usp. Fiz. Nauk* **113** 597 (1974) [*Sov. Phys. Usp.* **17** 497 (1974)]
11. Pokazan'ev V G, Skrotskiĭ G V *Usp. Fiz. Nauk* **107** 623 (1972) [*Sov. Phys. Usp.* **15** 230 (1972)]
12. Bashkin S (Ed.) *Beam-Foil Spectroscopy* (Berlin: Springer-Verlag, 1976)
13. Aleksandrov E B, Khvostenko G I, Chaĭka M P *Interferentsiya Atomnykh Sostoyaniĭ* (Interference of Atomic States) (Moscow: Nauka, 1991) [Translated into English (Berlin: Springer – Verlag, 1988)]
14. Berman P R (Ed.) *Atom Interferometry* (San Diego: Academic Press, 1997)
15. Lamb W E, Rutherford R C *Phys. Rev.* **72** 241 (1947); *Phys. Rev.* **79** 549 (1950) [Translated into Russian *Usp. Fiz. Nauk* **45** 553 (1951)]
16. Triebwasser S, Dayhoff E S, Lamb W E *Phys. Rev.* **89** 98 (1953)
17. Robiscoe R T, Shyn T W *Phys. Rev. Lett.* **24** 559 (1970)
18. Appelquist T, Brodsky S J *Phys. Rev. Lett.* **24** 562 (1970)
19. Sokolov Yu L *Zh. Eksp. Teor. Fiz.* **63** 461 (1972) [*Sov. Phys. JETP* **36** 243 (1973)]
20. Sokolov Yu L, in *Proc. 6th Int. Conf. on Atomic Physics* (Riga, 1978) p. 207
21. Donnally B L et al. *Phys. Rev. Lett.* **12** 502 (1964)
22. Gurevich A V, Pitaevskiĭ L P *Zh. Eksp. Teor. Fiz.* **46** 1281 (1964) [*Sov. Phys. JETP* **19** 870 (1964)]
23. Pais A, Piccioni O *Phys. Rev.* **100** 1487 (1955)
24. Sokolov Yu L *Pis'ma Zh. Eksp. Teor. Fiz.* **11** 524 (1970) [*JETP Lett.* **11** 359 (1970)]
25. Sokolov Yu L, Yakovlev V P *Zh. Eksp. Teor. Fiz.* **83** 15 (1982) [*Sov. Phys. JETP* **56** 7 (1982)]
26. Pal'chikov V G, Yakovlev V P, Sokolov Yu L *Physica Scripta* **55** 33 (1997)
27. Sokolov Yu L, in *Proc. 2nd Int. Conf. on Precision Measurements and Fundamental Constants II* (Gaithersberg, June 8 – 12, 1981) p. 135
28. Pal'chikov V G, Sokolov Yu L, Yakovlev V P *Metrologia* **21** 99 (1985)
29. Pal'chikov V G, Sokolov Yu L, Yakovlev V P *Pis'ma Zh. Eksp. Teor. Fiz.* **38** 347 (1983) [*JETP Lett.* **38** 418 (1983)]
30. Sokolov Yu L et al. *Nuovo Cimento* **14D** 183 (1992)
31. Sokolov Yu L, in *The Hydrogen Atom* (Eds G F Bassani, M Inguscio, T W Hänsch) (Berlin: Springer-Verlag, 1989) p. 16
32. Kadomtsev B B et al. *Physica Scripta* **54** 156 (1996)
33. Sokolov Yu L, Yakovlev V P, Pal'chikov V G *Laser Phys.* **3** 635 (1993)
34. Sokolov Yu L, Yakovlev V P, Pal'chikov V G *Physica Scripta* **49** 86 (1994)
35. Sokolov Yu L, in *Proc. IIIrd Workshop* "*Optics and Interferometry with Atoms*" (Italy, Elba Island, 1996) p. O-18
36. Kadomtsev B B *Usp. Fiz. Nauk* **164** 449 (1994) [*Phys. Usp.* **37** 425 (1994)]
37. Kadomtsev B B, Kadomtsev M B *Physica Scripta* **50** 243 (1994)
38. Kadomtsev B B, Kadomtsev M B *Zh. Eksp. Teor. Fiz.* **108** 1634 (1995) [*JETP* **81** 897 (1995)]
39. Kadomtsev B B *Phys. Lett. A* **210** 371 (1996)
40. Kadomtsev B B, Kadomtsev M B *Chaos* **6** 399 (1996)
41. Kadomtsev B B, Kadomtsev M B *Usp. Fiz. Nauk* **166** 651 (1996) [*Phys. Usp.* **39** 697 (1996)]
42. Kadomtsev B B *Dinamika i Informatsiya* (Dynamics and Information) (Moscow: Uspekhi Fizicheskikh Nauk, 1997); 2nd ed. (Moscow: Uspekhi Fizicheskikh Nauk, 1999)
43. Pal'chikov V G, Yakovlev V P, Sokolov Yu L *Physica Scripta* **55** 33 (1997)
44. May R M *Nucl. Fusion* **4** 207 (1964)